Validation of Doppler scatterometer concepts using measurements from the Black Sea Research Platform

<u>Yurovsky Yu. Yu.</u>, MHI RAS, Russia

Kudryavtsev V.N., MHI RAS, RSHU, Russia

Grodsky S.A., Maryland University, US

Chapron B., IFREMER, France

RSF | Russian Science Foundation

Supported by RCSF grant 17-77-10052

Marine Hydrophysical Institute

Oceanographic Platform

Motivation

- Doppler shifts linearly related to the surface velocity →

- Doppler scatterometer is a promising tool for the (satellite) **sea surface current** (SSC) monitoring

- Additional Doppler velocity measurements can be inverted to the SSC using GMF-based approach, similarly to the wind retrieval → A **GMF** for the Doppler velocity as well as its theory are required

- Switching to higher microwave bands (**Ka-band**) allow to increase Doppler velocity accuracy measurements → planned missions: DoppScatt, SKIM

[Goldstein & Zebker, 1987, Nat.],
[Romeiser & Thompson, 2000, TGRS],
[Chapron et al., 2005, JGR], [Ardhuin et al. 2017, OSD],
[Bao et al. 2017, TGRS], [Rodriguez et al., 2018, RS]

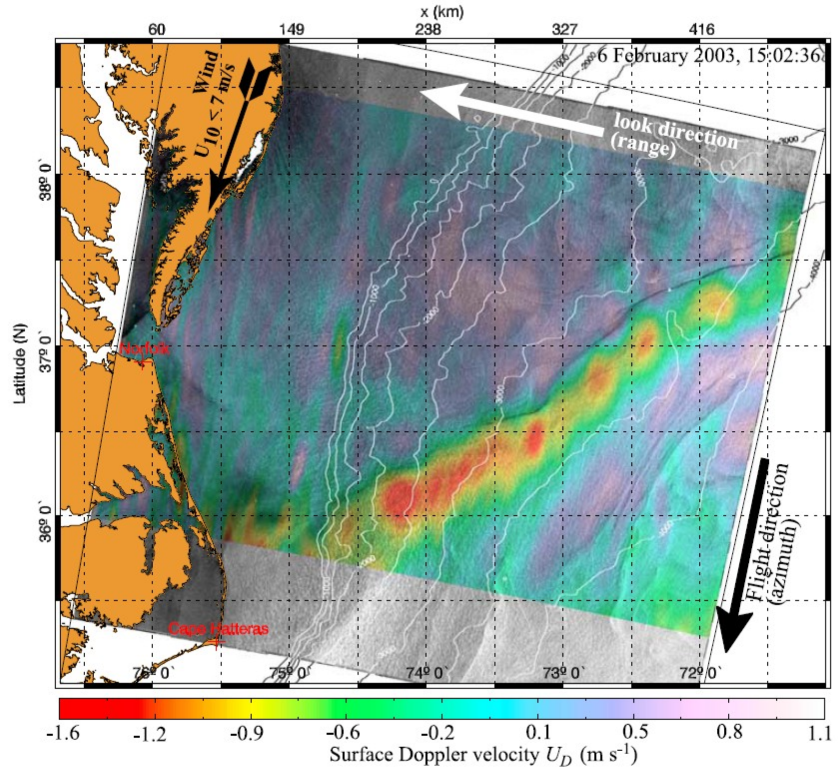

Figure 1. Normalized radar cross-section σ_0 (gray shades) and Doppler velocity U_D (colors), analyzed from a wide-swath image obtained by ENVISAT on 6 February 2003 at 1512 UTC. Oceanic fronts appear as sharp gradients of σ_0, while the surface velocity seen by the radar appears to be related to the Gulf Stream.

[Chapron, Collard, Ardhuin, 2005, JGR]

Doppler Velocity of the Sea Surface

Geophysical Doppler anomaly (centroid of time/space-resolved Doppler specrum):

$$v = ([\mathbf{v}_c + \mathbf{v}_s + \overline{\sigma' \mathbf{u}'}/\overline{\sigma}] \cdot \mathbf{k}_r)/|\mathbf{k}_r|,$$

v_c is the surface current velocity
v_s is the scatterer velocity in terms of two-scale model
σ’ is the NRCS variation
u’ is the orbital velocity component
k_r is the radar wave number

+ Approaching
- Receding

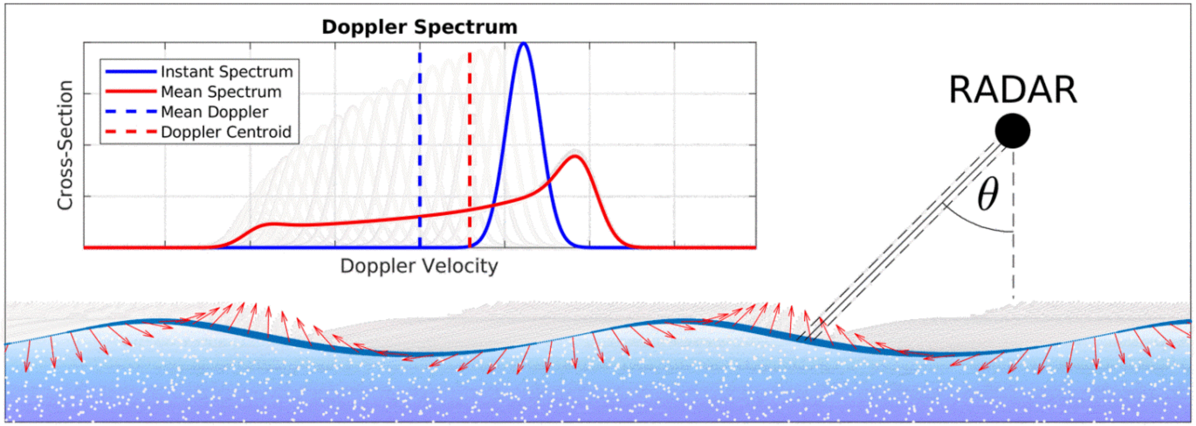

Marine Hydrophysical Institute Russian Acad. Sci. (MHI RAS) Research Platform

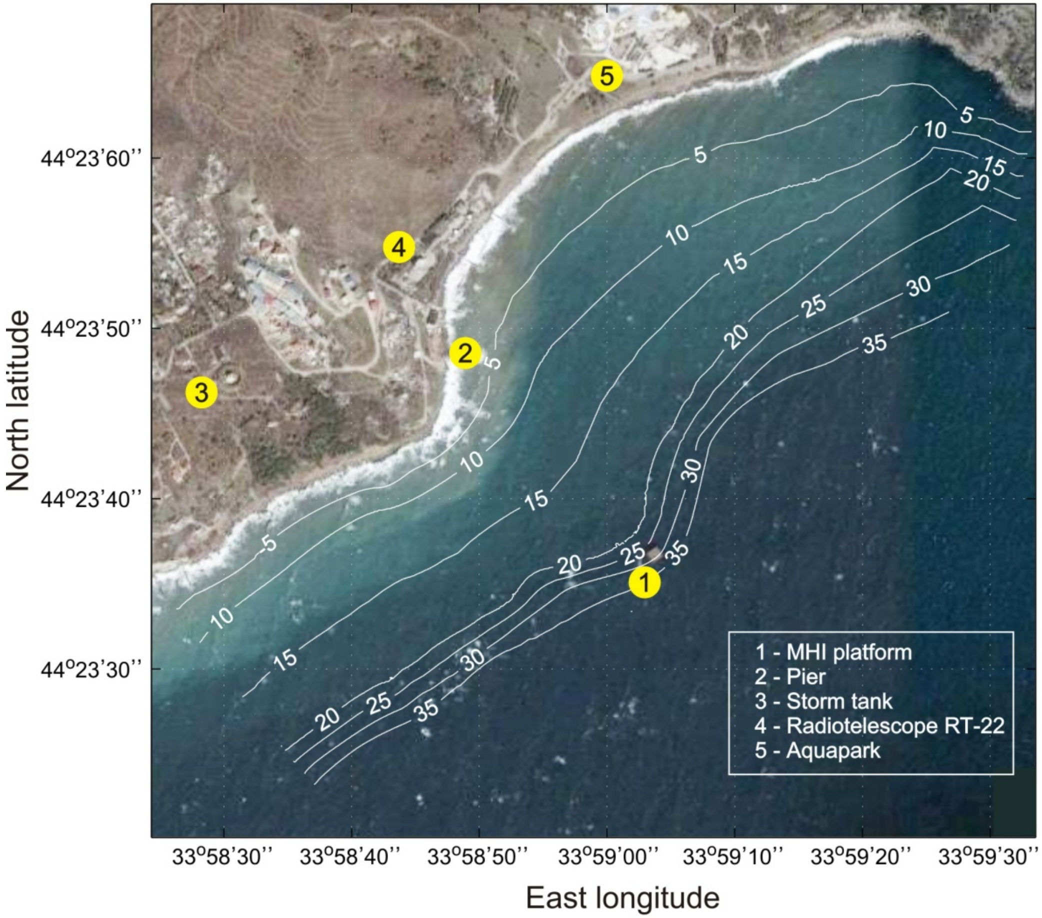

MHI RAS Research platform

Wavelength upto 60 m at U=20 m/s

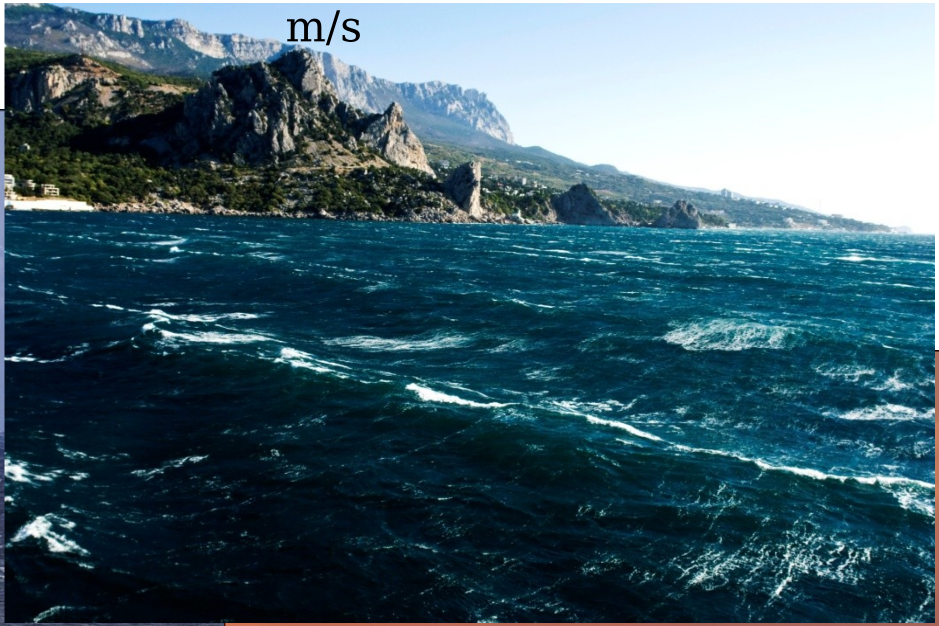

Instruments

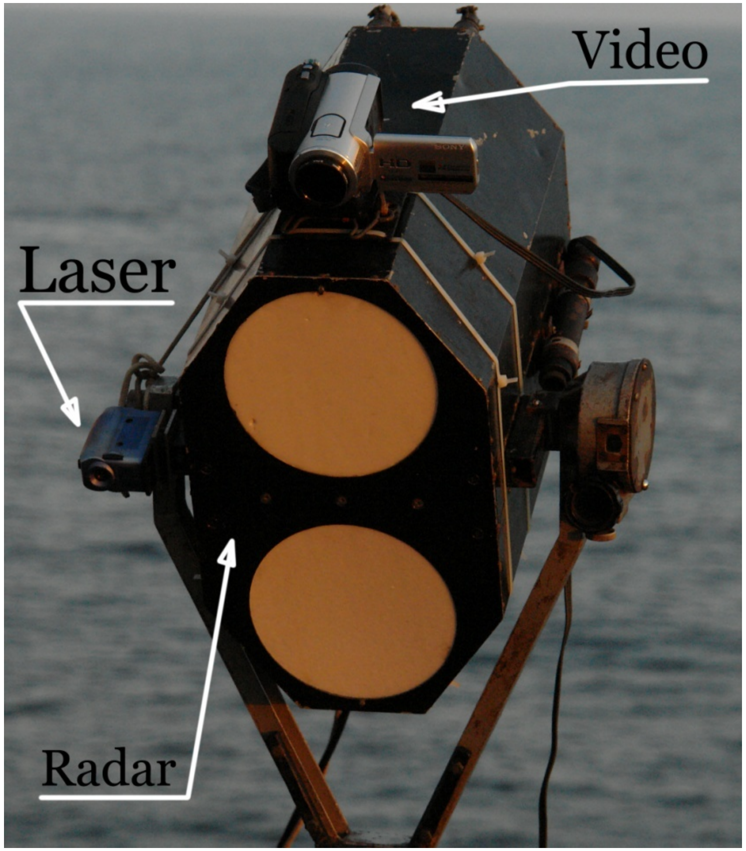

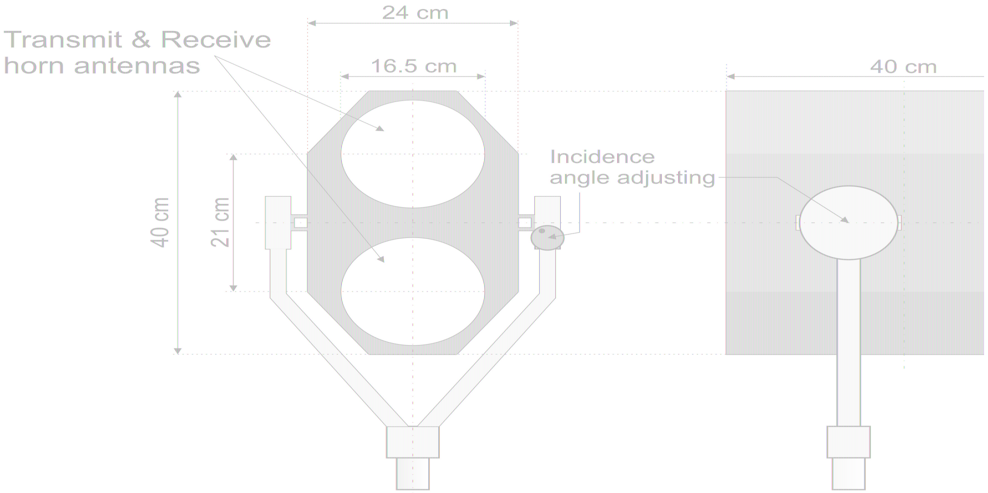

Type	CW Doppler Scatterometer
Polarization	VV,HH
Wavelength, Freq.	8 mm, 37.5GHz
CW Power	100 mW
Antenna	Conical horns for Tx and Rx

+ meteo station, wire wave gauge, videocamera, submerged current sensors

Measurements

The measurements are carried out in 2009 - now.

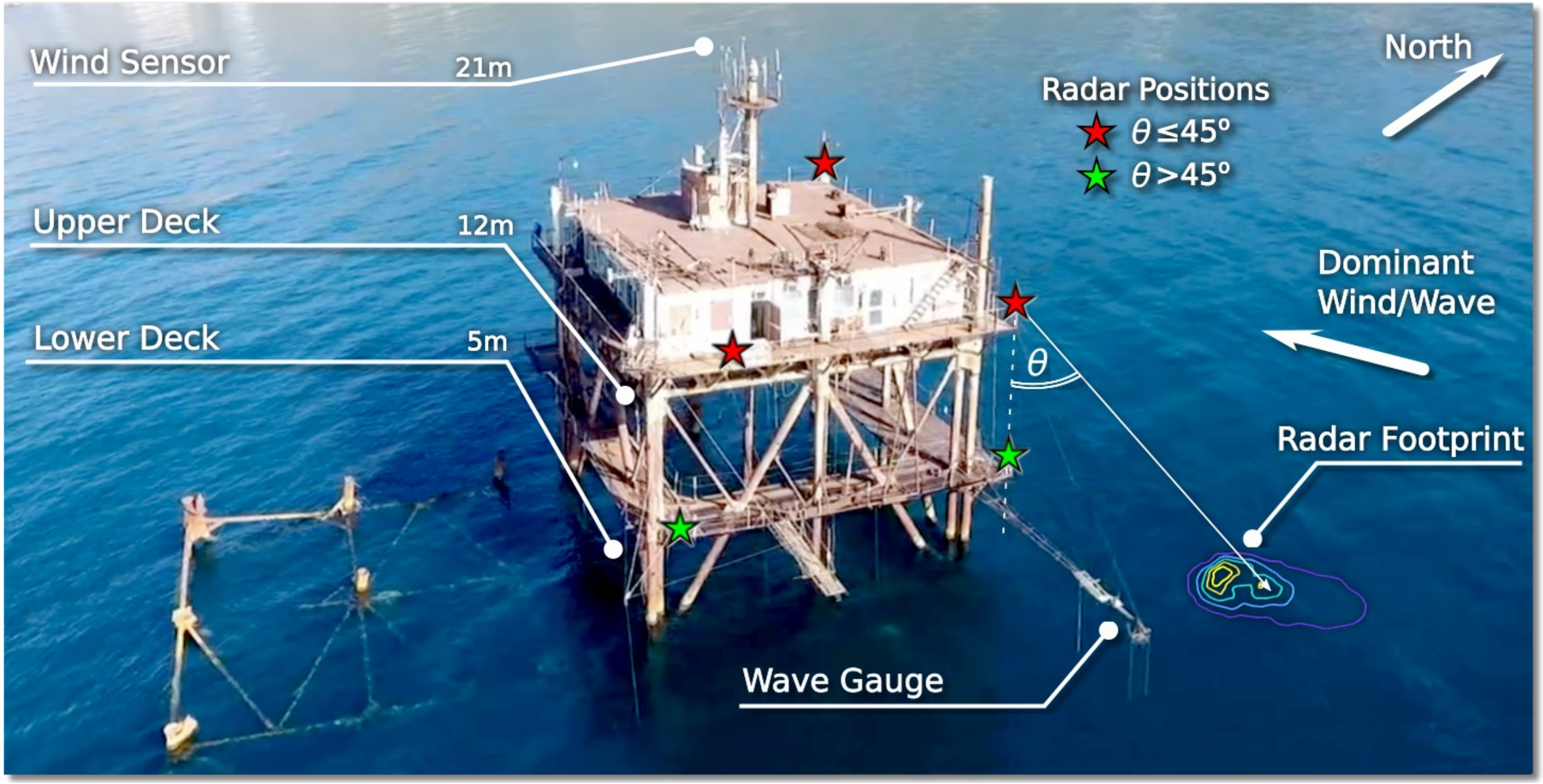

Measurements

Data samples distributions over incidence angle, azimuth, and wind speed.

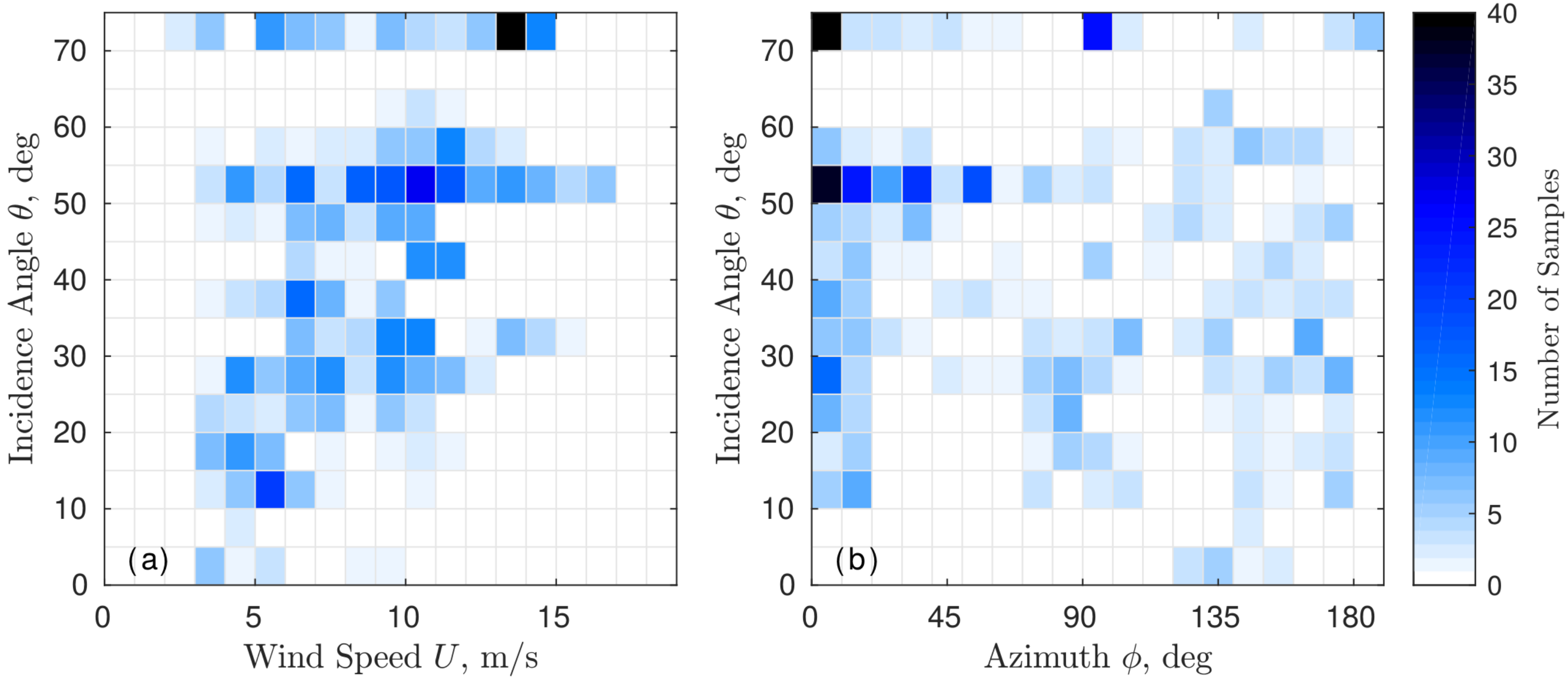

Contents

1. Mean levels of NRCS
2. Modulation of NRCS
3. Breaking wave manifestation
4. Doppler properties estimates

The NRCS Model function

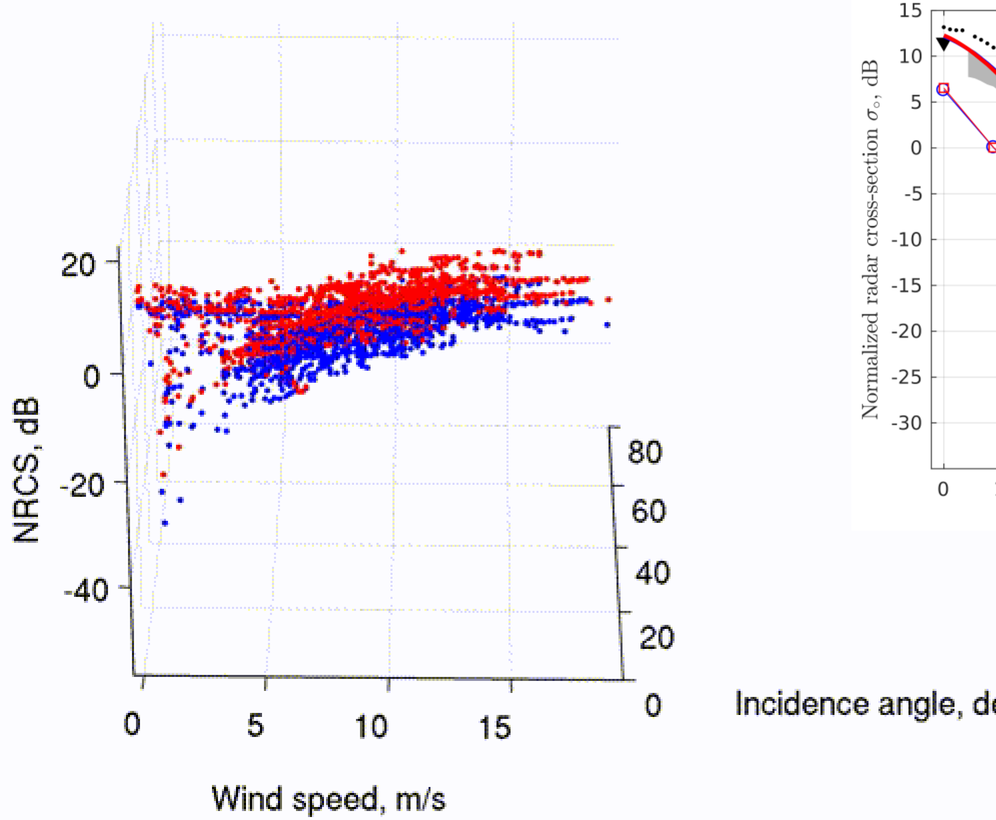

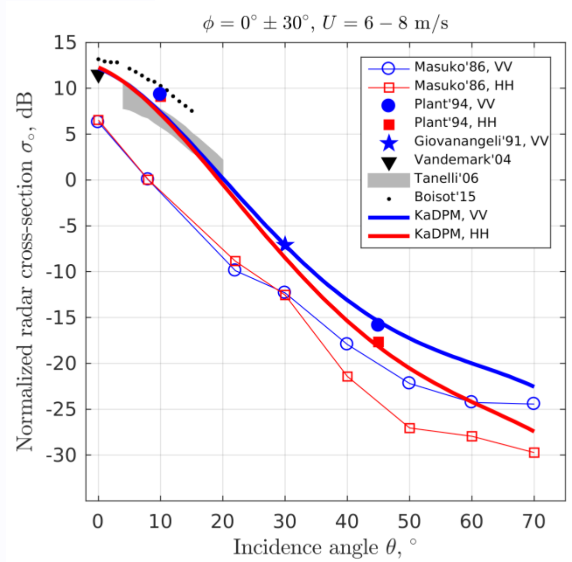

[Y. Y. Yurovsky, V. N. Kudryavtsev, S. A. Grodsky, and B. Chapron, “Ka-Band Dual Copolarized Empirical Model for the Sea Surface Radar Cross Section,” IEEE Transactions on Geoscience and Remote Sensing, vol. 55, no. 3, pp. 1629–1647, 2017]

NRCS Model (KaDPM)

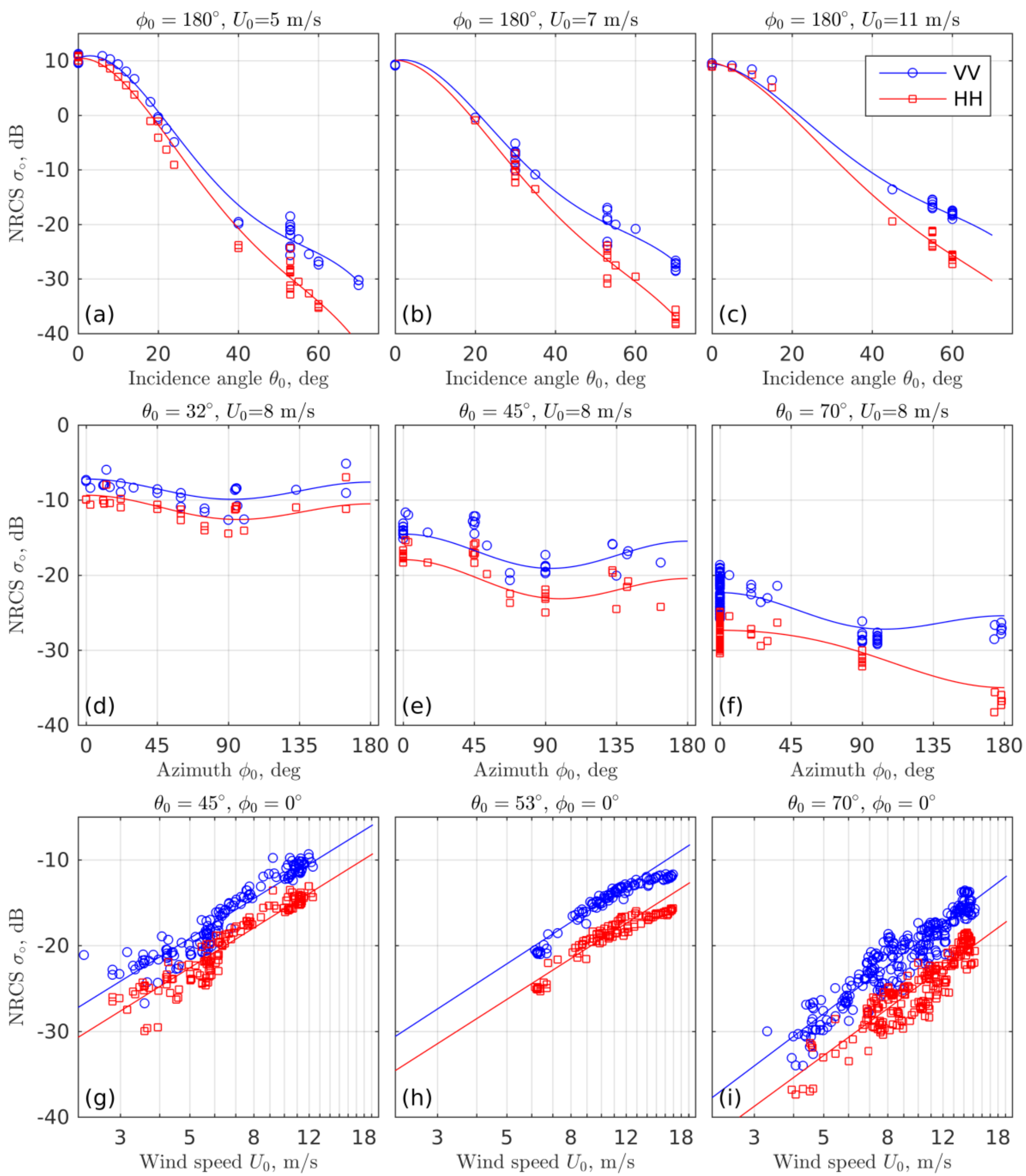

- Points – measurements
- Lines – polynomial fit
- Standard 2-harmonic azimuthal spreads
- Some sort of saturation at winds > 15 m/s
- Pure measurements suffer from antenna impacts (different at VV and HH) → "weird" polarization ratio at small incidence angles

Data fitting. Antenna pattern correction

$$\sigma_{\text{oeff}}(\theta_0, \phi_0, U) = \frac{\int \Gamma_{\text{eff}}(x,y)\sigma_\text{o}(x,y,U)\mathrm{d}x\mathrm{d}y}{\int \Gamma_{\text{eff}}(x,y)\mathrm{d}x\mathrm{d}y} = \quad (4)$$

$$= \frac{\int \Gamma_{\text{eff}}(\theta,\phi)\sigma_\text{o}(\theta,\phi,U)J(\theta,\phi)\mathrm{d}\theta\mathrm{d}\phi}{\int \Gamma_{\text{eff}}(\theta,\phi)J(\theta,\phi)\mathrm{d}\theta\mathrm{d}\phi},$$

$$\log \sigma_\text{o} = A_0(\theta,U) + A_1(\theta,U)\cos\phi + A_2(\theta,U)\cos 2\phi, \quad (6)$$

$$A_j = \sum_{m=0}^{4}\sum_{k=0}^{1} C_{mjk}\theta^m(\log U)^k, \quad (7)$$

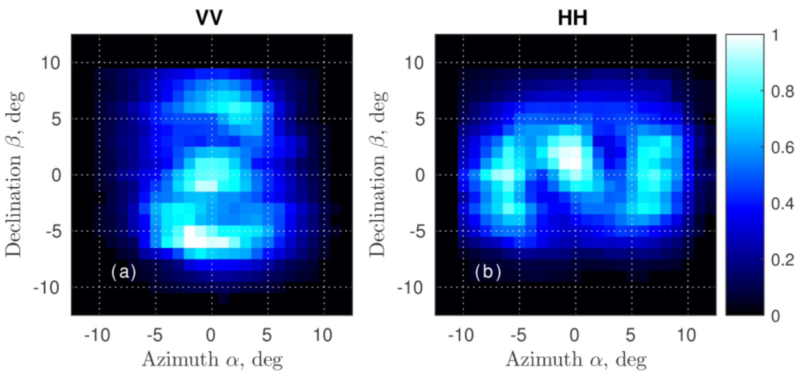

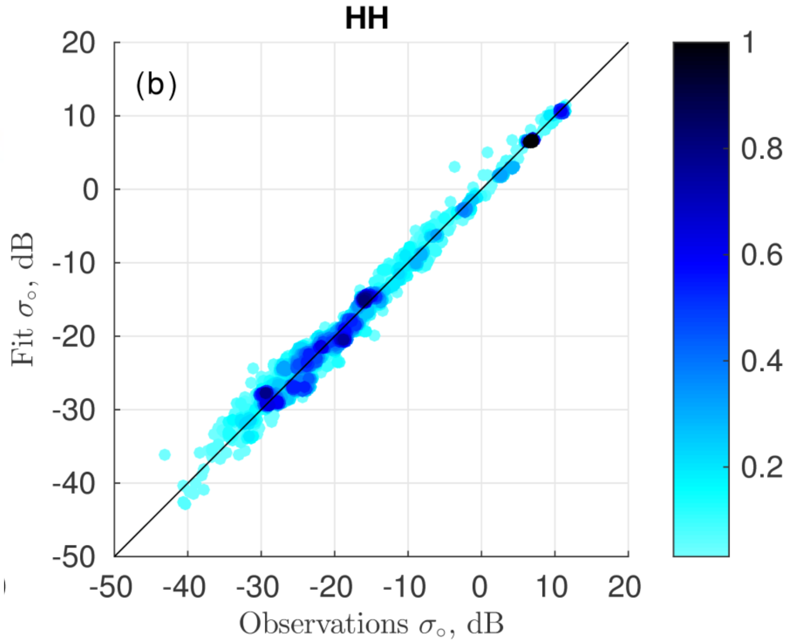

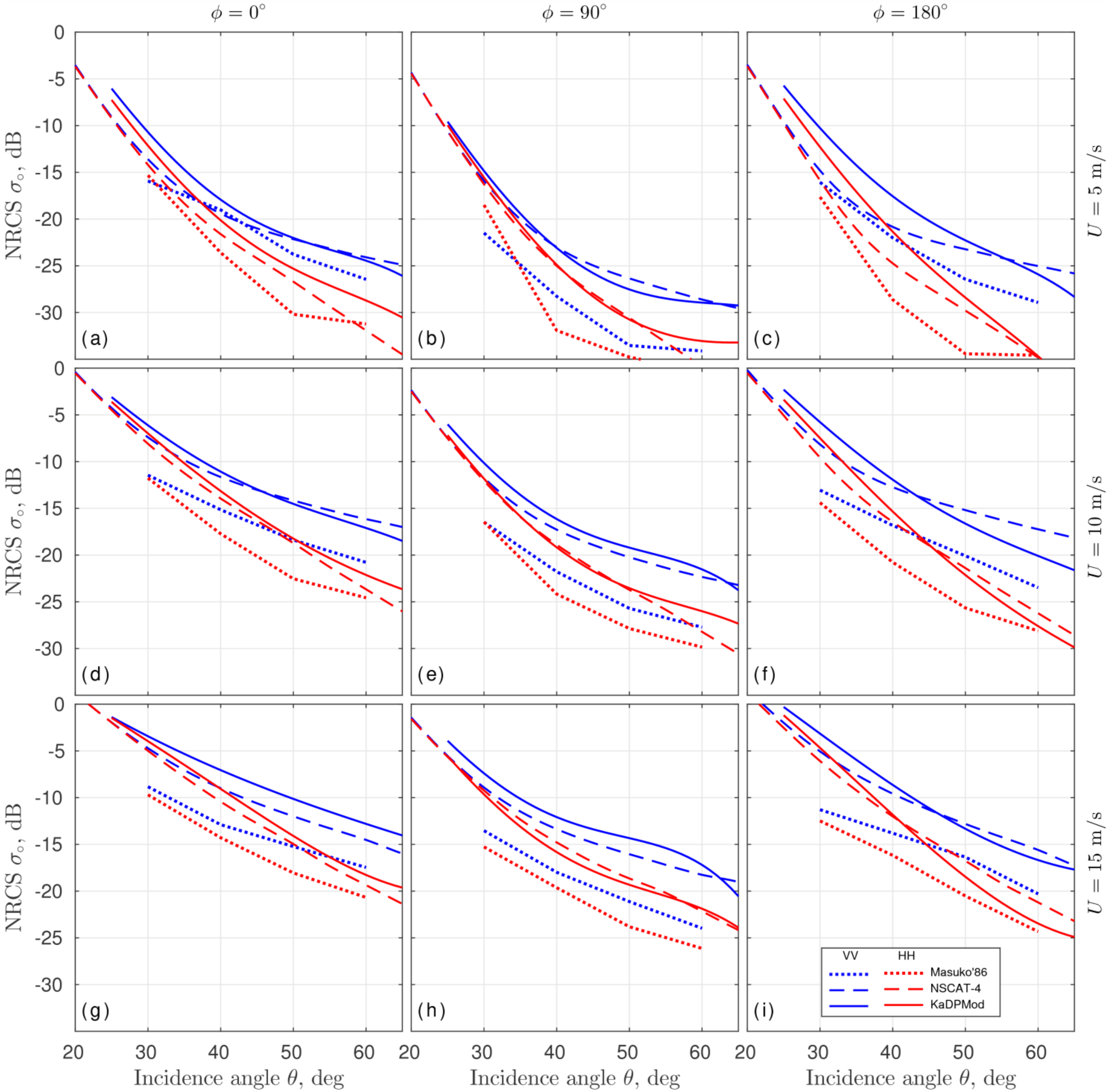

- After correction the fits are more reliable
- Our Ka-band data (KaDPM) is quite close to Ku-band (NSCAT-4)
- Data by [Masuko et al. 1986] are much lower

Contents

1. Mean levels of NRCS
2. Modulation of NRCS
3. Breaking wave manifestation
4. Doppler properties estimates

Doppler Signal Time Series

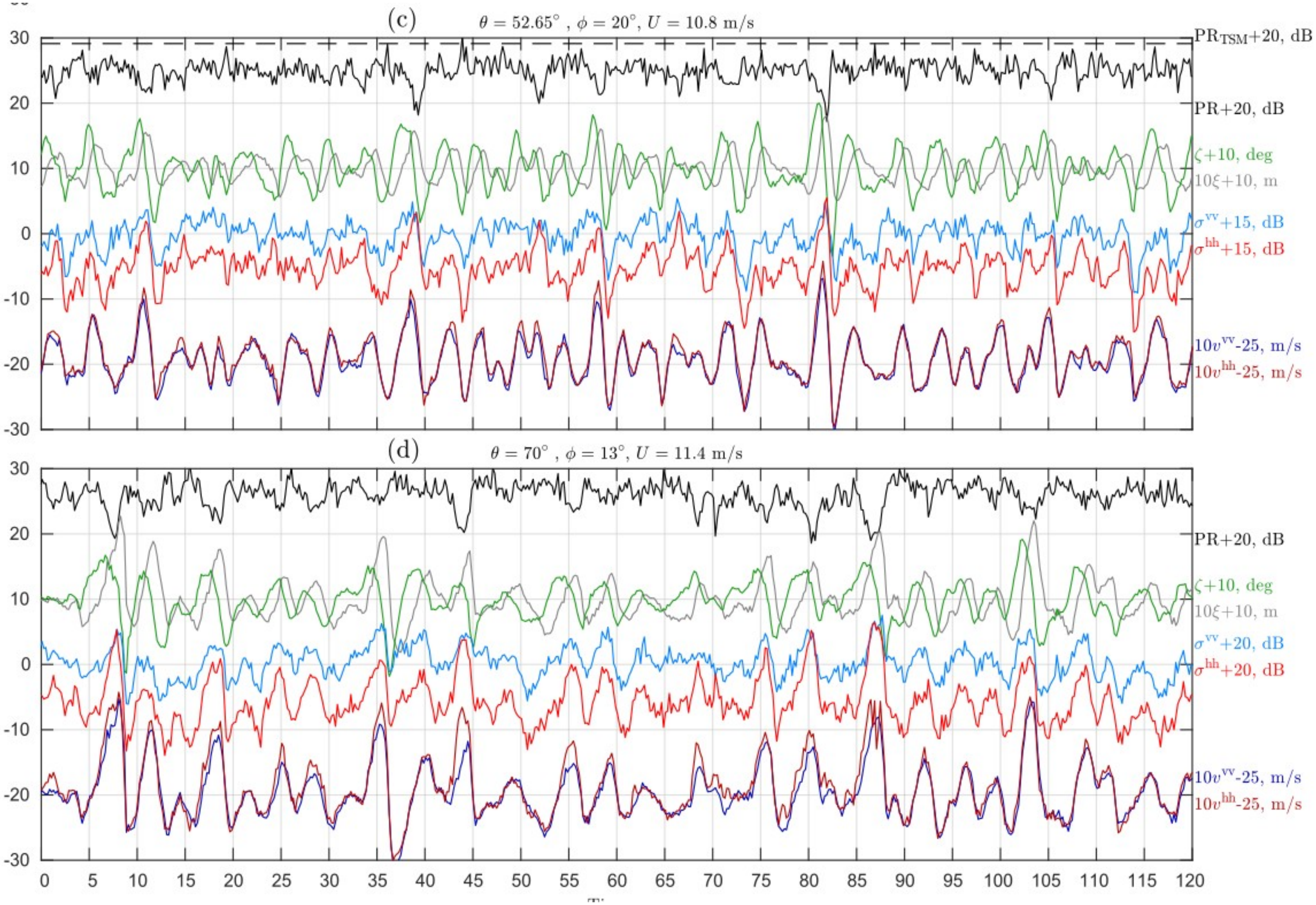

- DV spikes are much weaker than the NRCS spikes
- DV spikes presumably are the PHASE velocities of breakers [Jessup et al. 1991, Hansen et al. 2012]
- DV spike corresponds to the phase velocities of waves much shorter than peak waves
- Peak waves do not break [Plant 2012, GRL]

Modulation Transfer Function

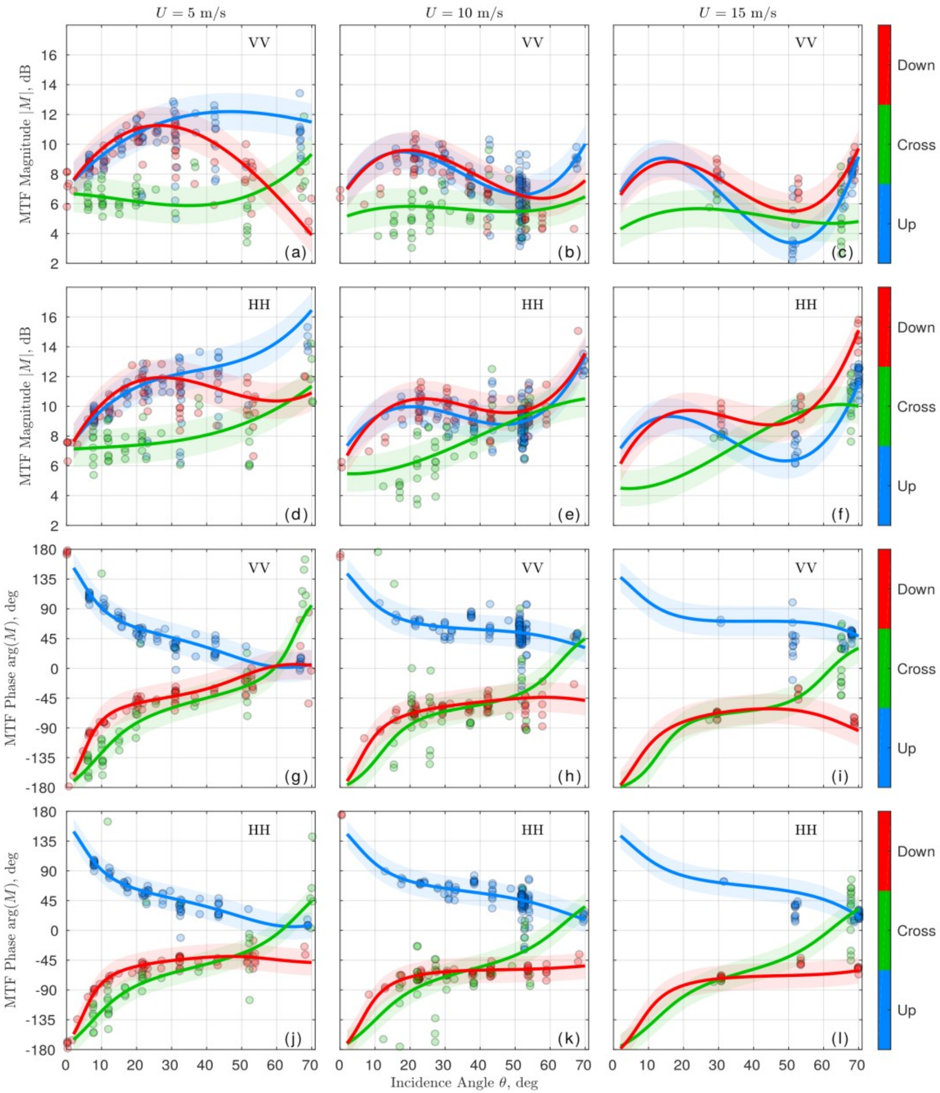

- MTF reflects the distribution of NRCS variation over the long wave profile

$$M = \frac{\sigma'}{\bar{\sigma} a k} = \frac{gG}{\bar{\sigma}\omega}\frac{S_{\sigma v}}{S_{vv}}$$

$$G = \cos\phi \sin\theta + i\cos\theta$$

- NRCS peaks at the front slope in upwind direction, and at the rear slope in downwind direction

- MTF magnitude has a peak at 20-30°, and increases after 65°.

$$\frac{\overline{v'\sigma'}}{\bar{\sigma}} = \mathrm{Re}\int g^{-1} G^{*} \omega^{3} M S_{zz} \mathrm{d}\omega$$

[Y. Y. Yurovsky, V. N. Kudryavtsev, B. Chapron, and S. A. Grodsky "Modulation of Ka-Band Doppler Radar Signals Backscattered From the Sea Surface", IEEE Transactions on Geoscience and Remote Sensing, vol. 56, no. 5, pp. 2931-2948, 2018]

Modulation Transfer Function

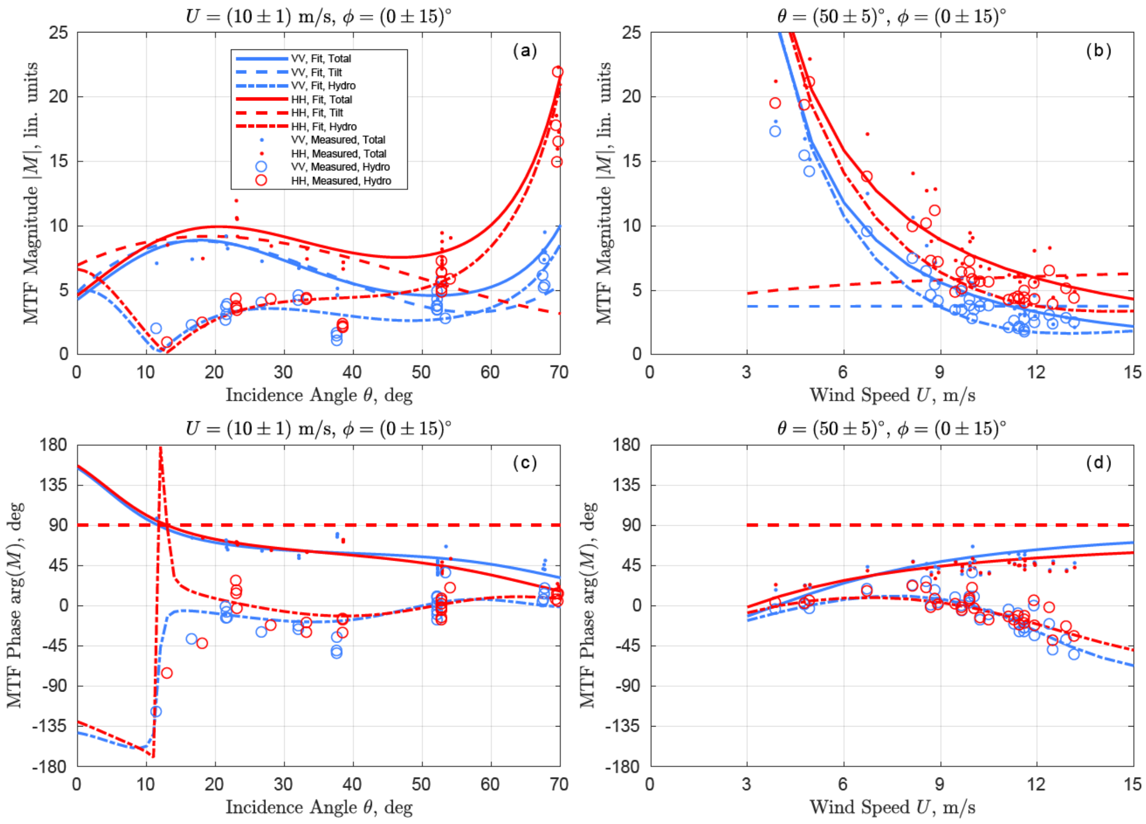

- Contrast inversion at 12-13 deg → Hydro-MTF flip
- This is close to SKIM incidence angle → weakest wind variability → better discrimination between wind-sea/slicks/ships etc.

[Y. Y. Yurovsky, V. N. Kudryavtsev, B. Chapron, and S. A. Grodsky "Modulation of Ka-Band Doppler Radar Signals Backscattered From the Sea Surface", IEEE Transactions on Geoscience and Remote Sensing, vol. 56, no. 5, pp. 2931-2948, 2018]

Contents

1. Mean levels of NRCS
2. Modulation of NRCS
3. Breaking wave manifestation
4. Doppler properties estimates

Simultaneous Radar & Video Measurements

Radar incidence angle = 53°, Camera incidence angle = 30°, Wind Speed = 11 m/s, SWH = 0.8 m

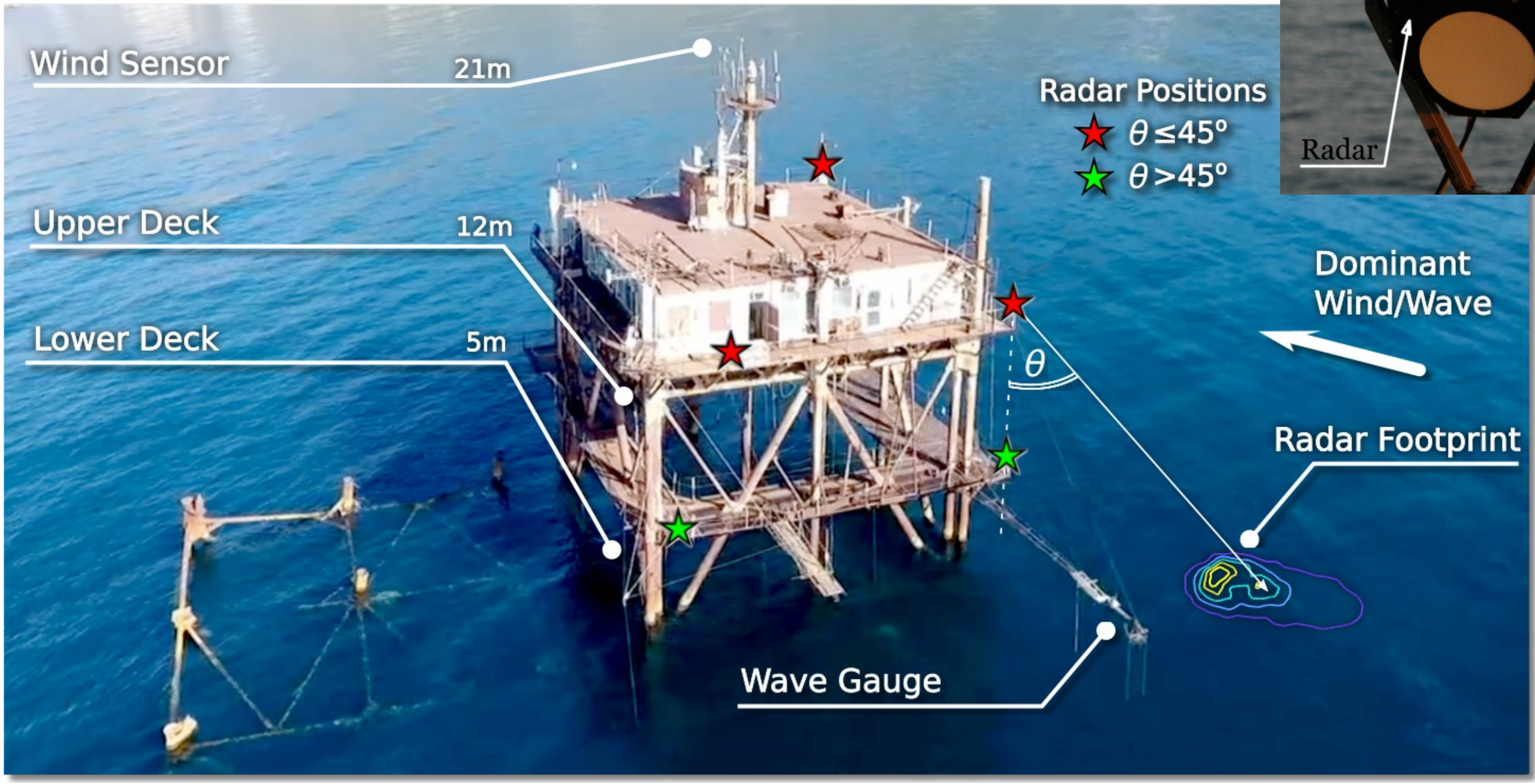

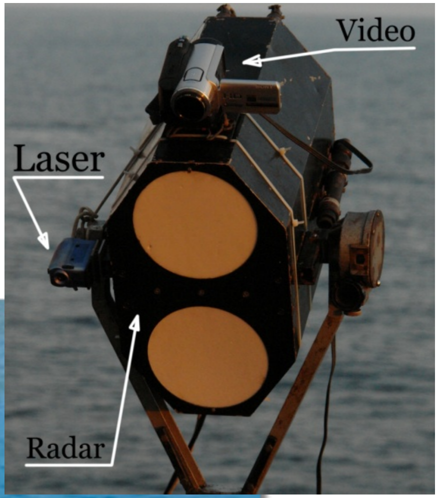

Data Processing

- 1) Select spikes in the HH-pol signal
- 2) Find corresponding frames in the video sequence (via audio data synchronization)
- 3) Estimate manually positions of rear and front edges of the breaker
- 4) Transform pixel coordinates into the flat surface coordinates
- 5) Estimate max/min/mean levels for each breaking wave event
  (line-of-sight projections, sinθ)
- 6) Compare Optical and Doppler Velocity of the breakers

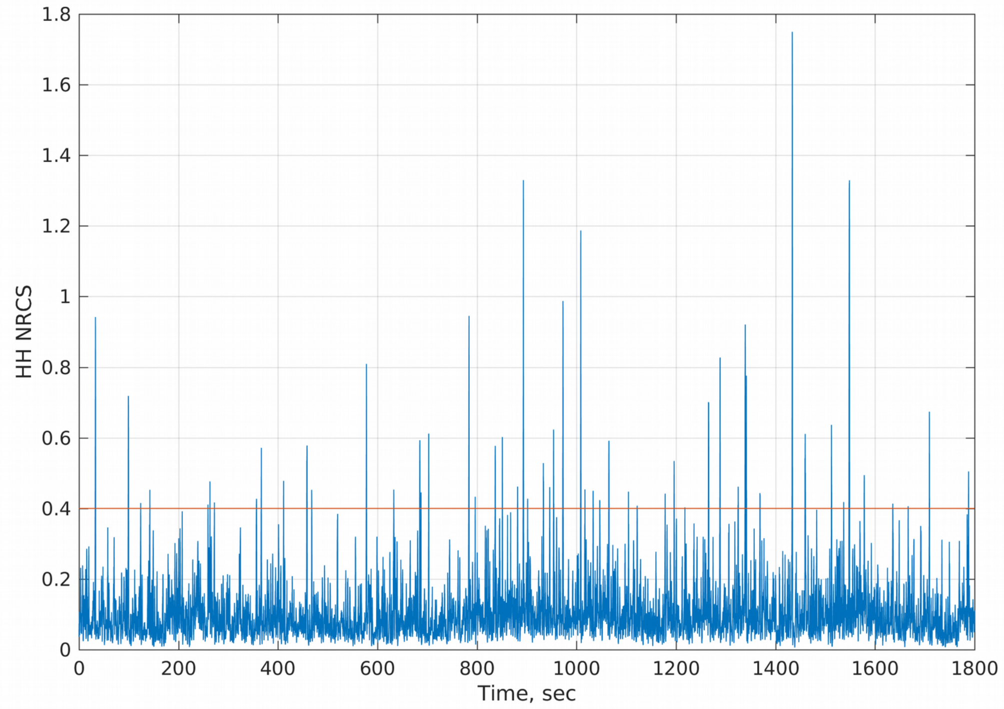

Data Processing

- 1) Select spikes in the HH-pol signal
- 2) Find corresponding frames in the video sequence (via audio data synchronization)
- 3) Estimate manually positions of rear and front edges of the breaker
- 4) Transform pixel coordinates into the flat surface coordinates
- 5) Estimate max/min/mean levels for each breaking wave event
  (line-of-sight projections, sinθ)
- 6) Compare Optical and Doppler Velocity of the breakers

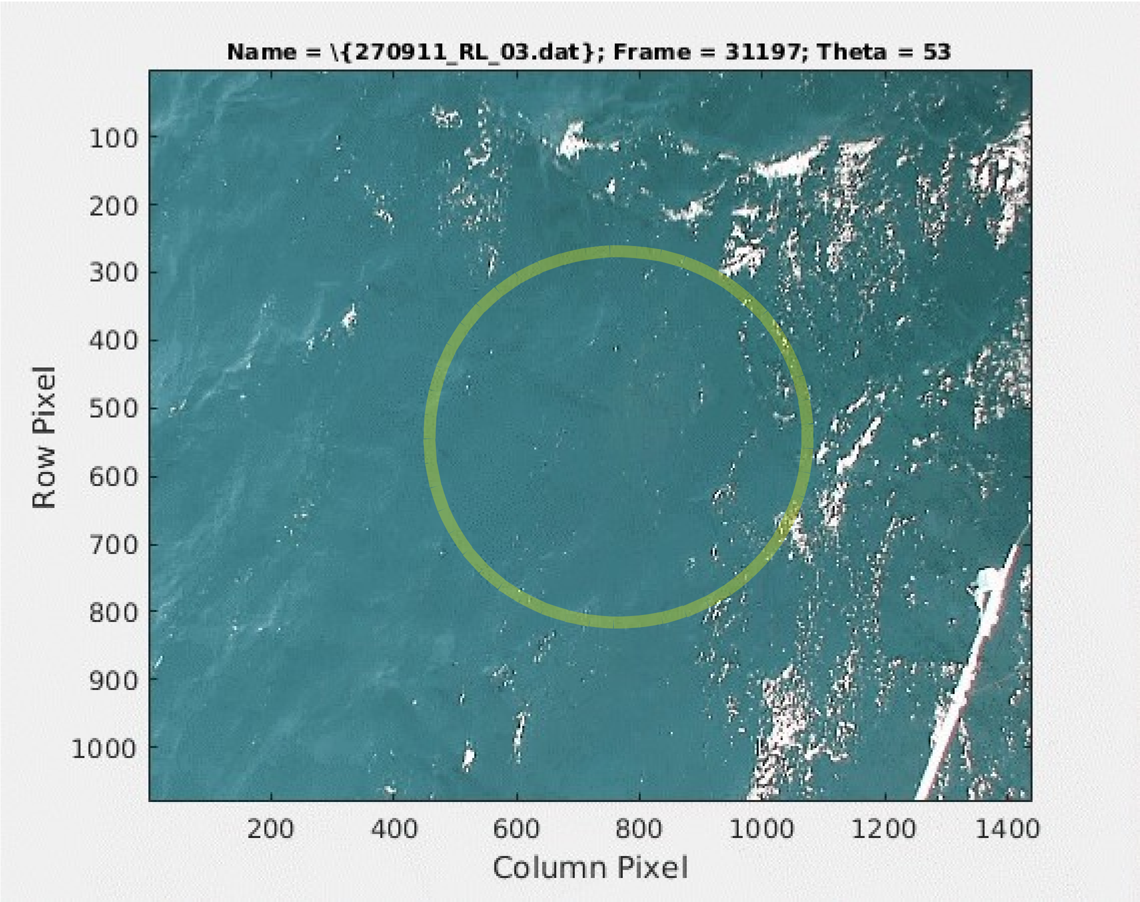

Data Processing

- 1) Select spikes in the HH-pol signal
- 2) Find corresponding frames in the video sequence (via audio data synchronization)
- <u>3) Estimate manually positions of rear and front edges of the breaker</u>
- 4) Transform pixel coordinates into the flat surface coordinates
- 5) Estimate max/min/mean levels for each breaking wave event

  (line-of-sight projections, sinθ)
- 6) Compare Optical and Doppler Velocity of the breakers

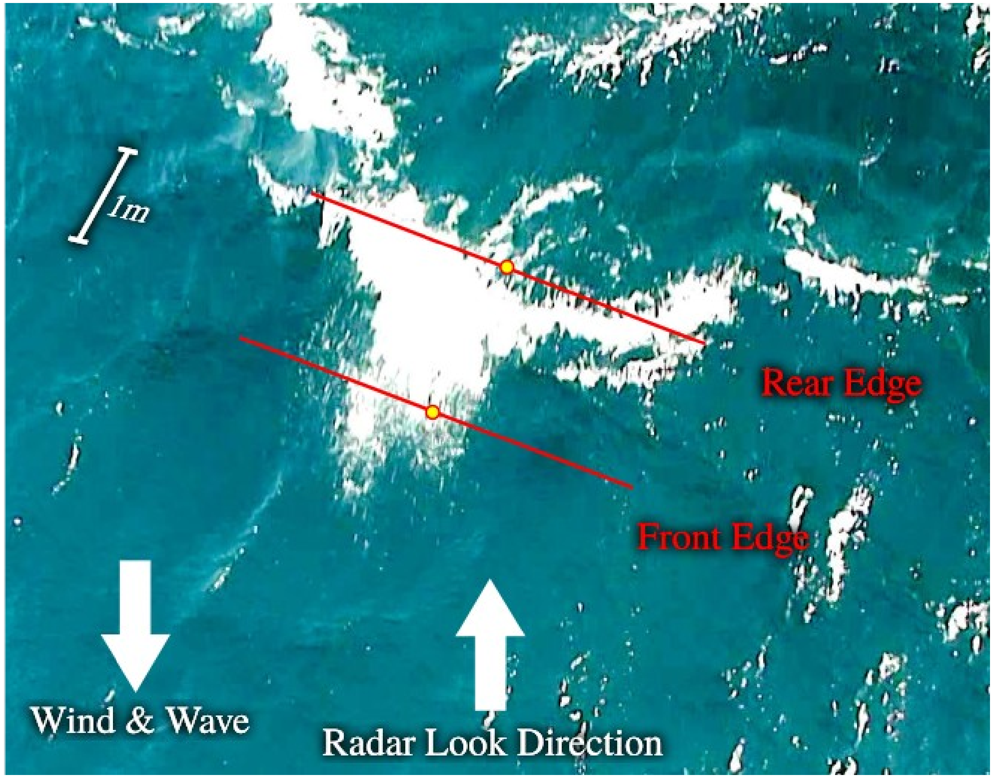

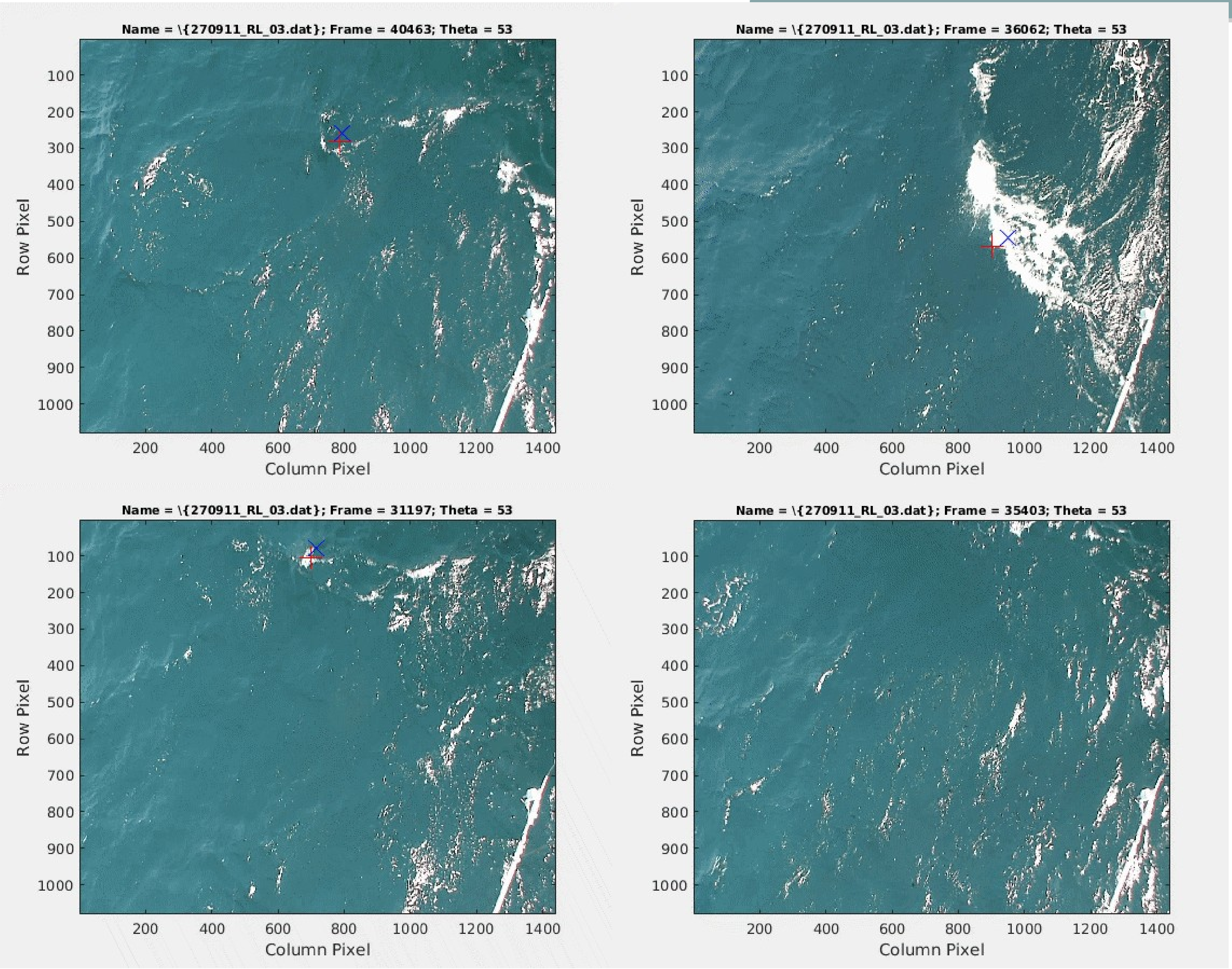

Name = \{270911_RL_03.dat}; Frame = 40463; Theta = 53
Name = \{270911_RL_03.dat}; Frame = 36062; Theta = 53
Name = \{270911_RL_03.dat}; Frame = 31197; Theta = 53
Name = \{270911_RL_03.dat}; Frame = 35403; Theta = 53
Row Pixel
Column Pixel
100
200
300
400
500
600
700
800
900
1000
200
400
600
800
1000
1200
1400

Results

No breaker

… increasing breaker intensity …

Cross-look

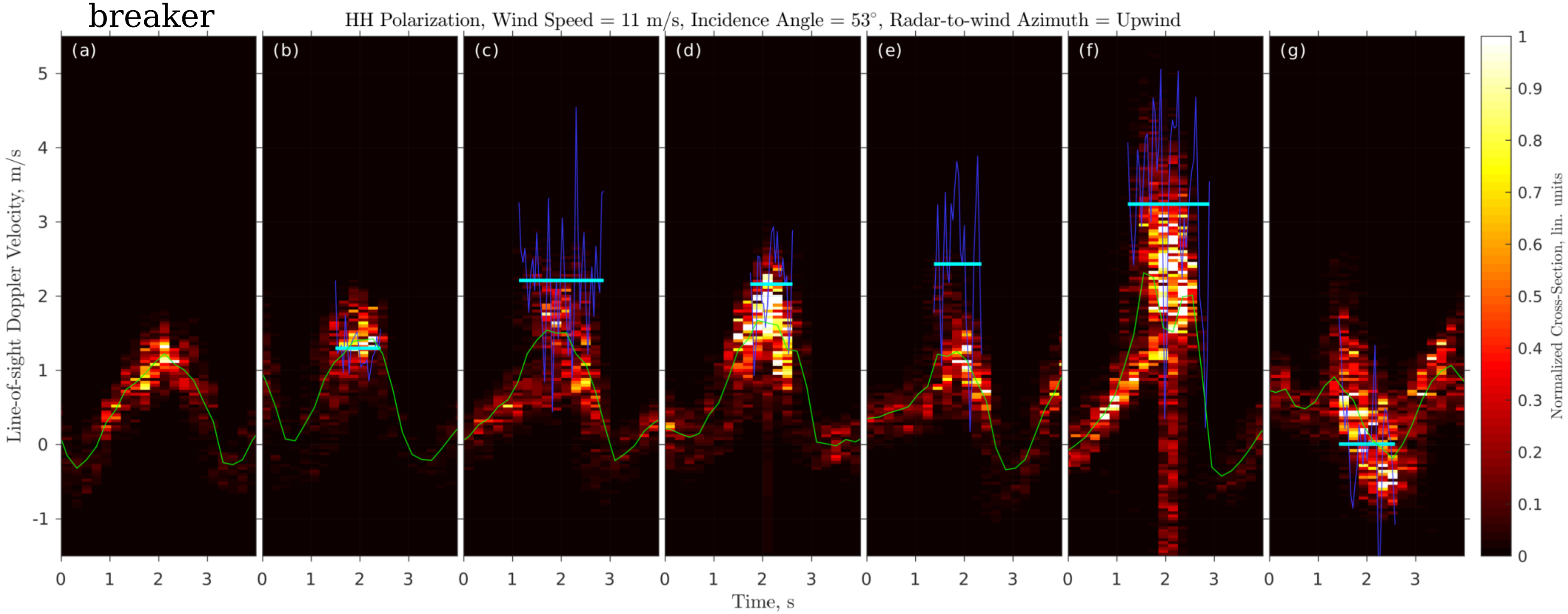

into the flat surface coordinates

- 5) <u>Estimate max/min/mean levels for each breaking wave event</u>
  (line-of-sight projections, sinθ)

- Green line – instantaneous Doppler centroid
- Blue line – instantaneous breaker velocity
- Cyan line – mean breaker velocity

Results

- 1) Select spikes in the HH-pol signal
- 2) Find corresponding frames in the video sequence (via audio data synchronization)
- 3) Estimate manually positions of rear and front edges of the breaker
- 4) Transform pixel coordinates into the flat surface coordinates
- 5) Estimate max/min/mean levels for each breaking wave event

  (line-of-sight projections, sinθ)
- 6) Compare Optical and Doppler Velocity of the

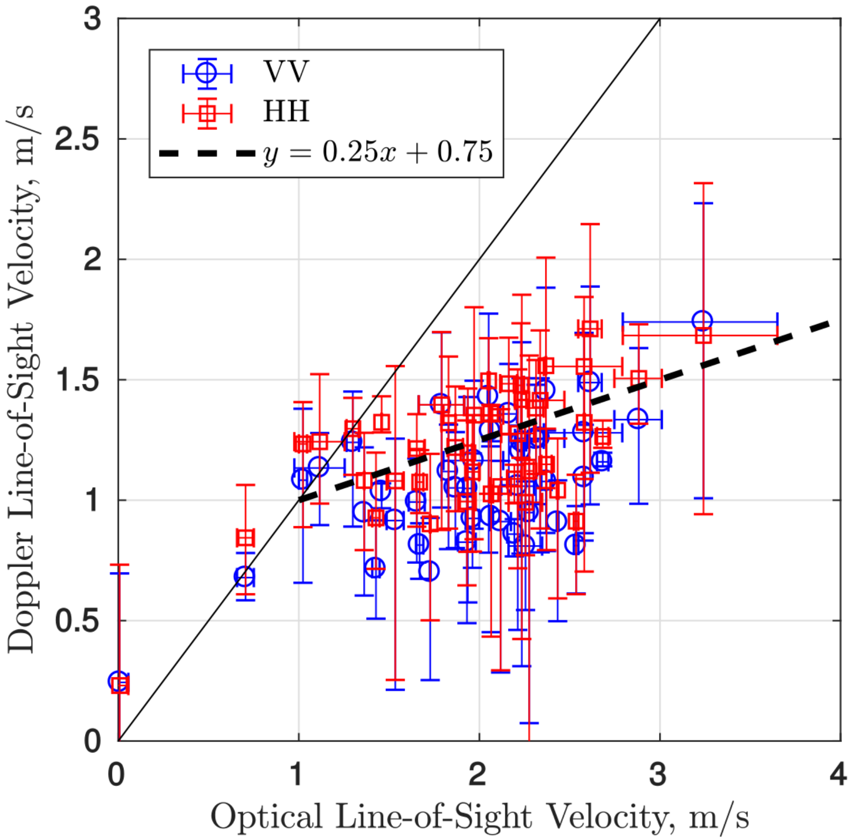

- $U_{\text{orbital}} = ak\ c_{\text{phase}} \sim 0.25\ c_{\text{phase}}$
- Breaking wave slope ~ 15 deg [Caulliez 2002, Kosnik & Dulov 2011]

Contents

Doppler Bandwidths

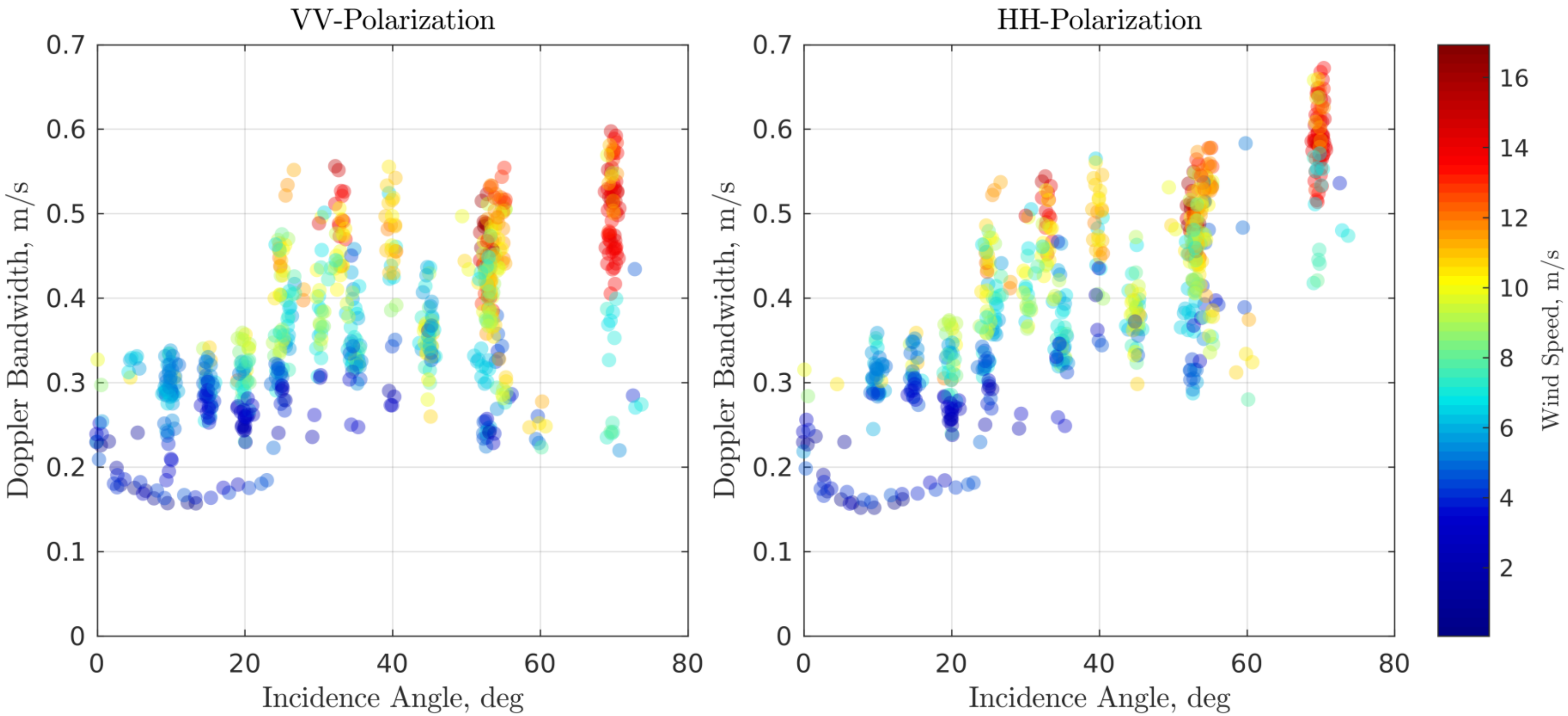

- Doppler Bandwidth is a function sea state mostly related to waves (orbital velocities)
- HH Bandwidth increases at large incidence angles > 60 deg indicating excessive Doppler velocities thanks to breakers
- At low incidence angles there is a gap in the dataset

Doppler Bandwidths

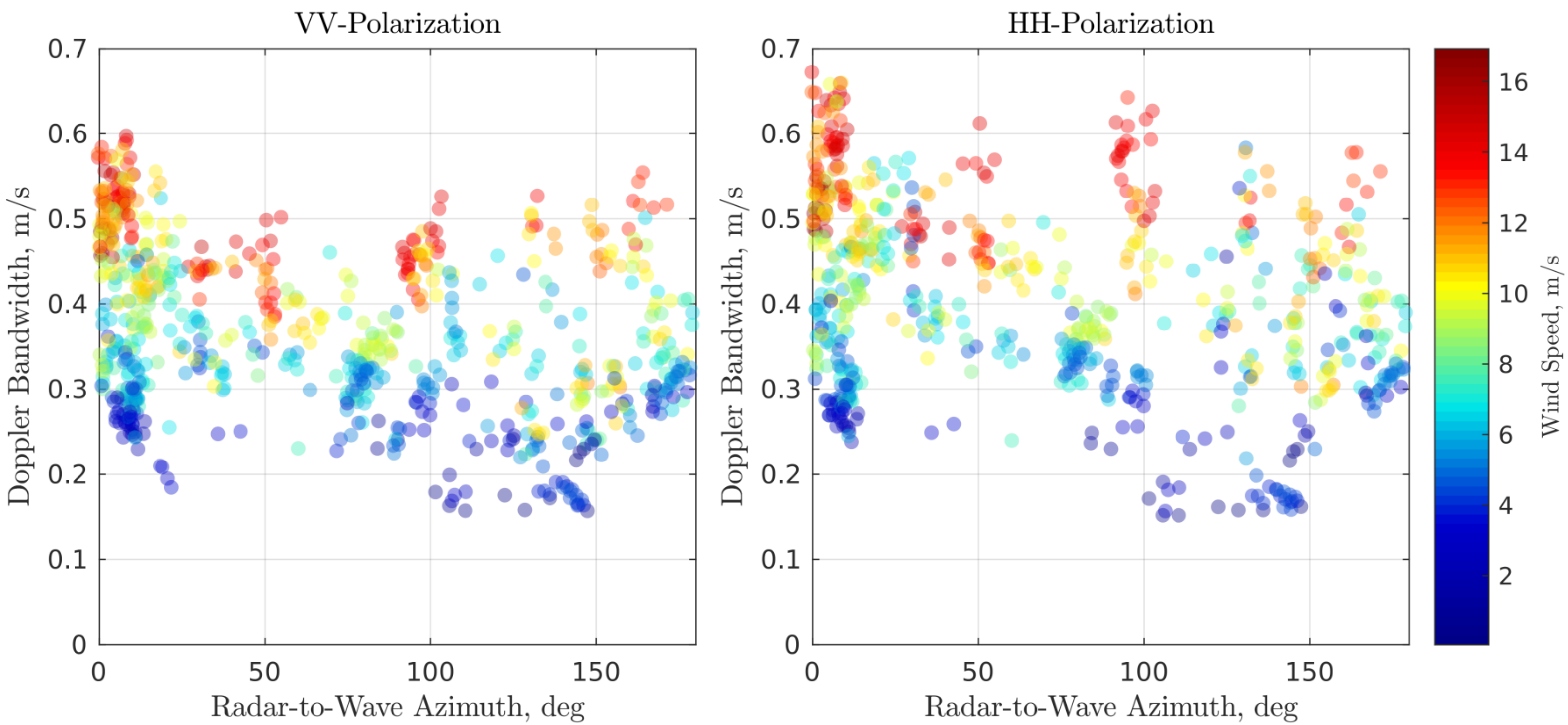

- In azimuth there is now strong bandwidth variability

Doppler Bandwidths vs Centroids

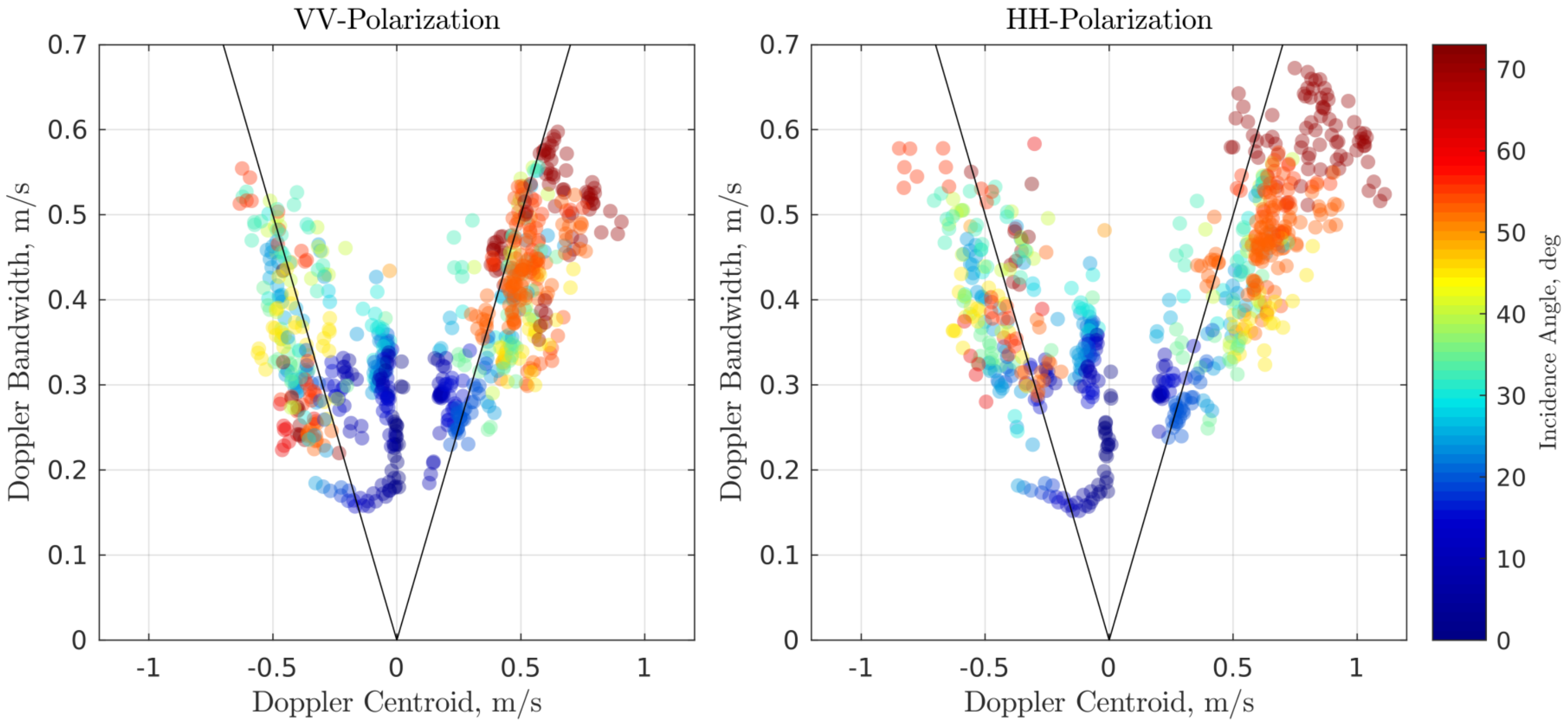

- Doppler bandwidths and Doppler centroids are closely related indicating Rayleigh-like shape of the Doppler spectrum
- Again, increasing deviations are seen at large theta and HH polarization

Doppler Centroids

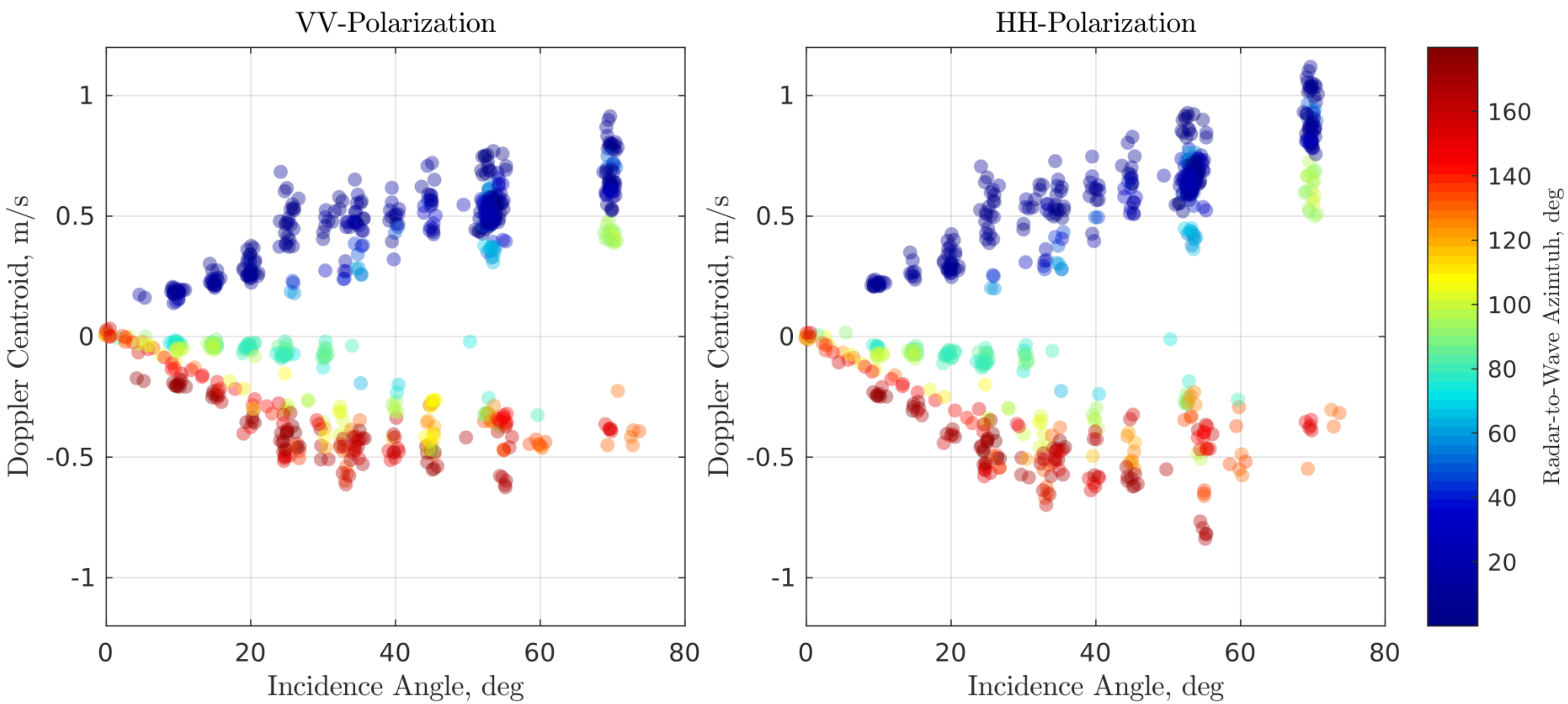

- Doppler centroid is a function of incidence angle, radar-to-wave azimuth, and sea state (waves)
- Some sort of saturation in incidence angle is evident in downwind, while there is a strong incidence angle trend in upwind → breakers?
- Non-zero (positive) cross-wave Doppler centroid at large incidence angle → hydro-MTF

Doppler Centroids

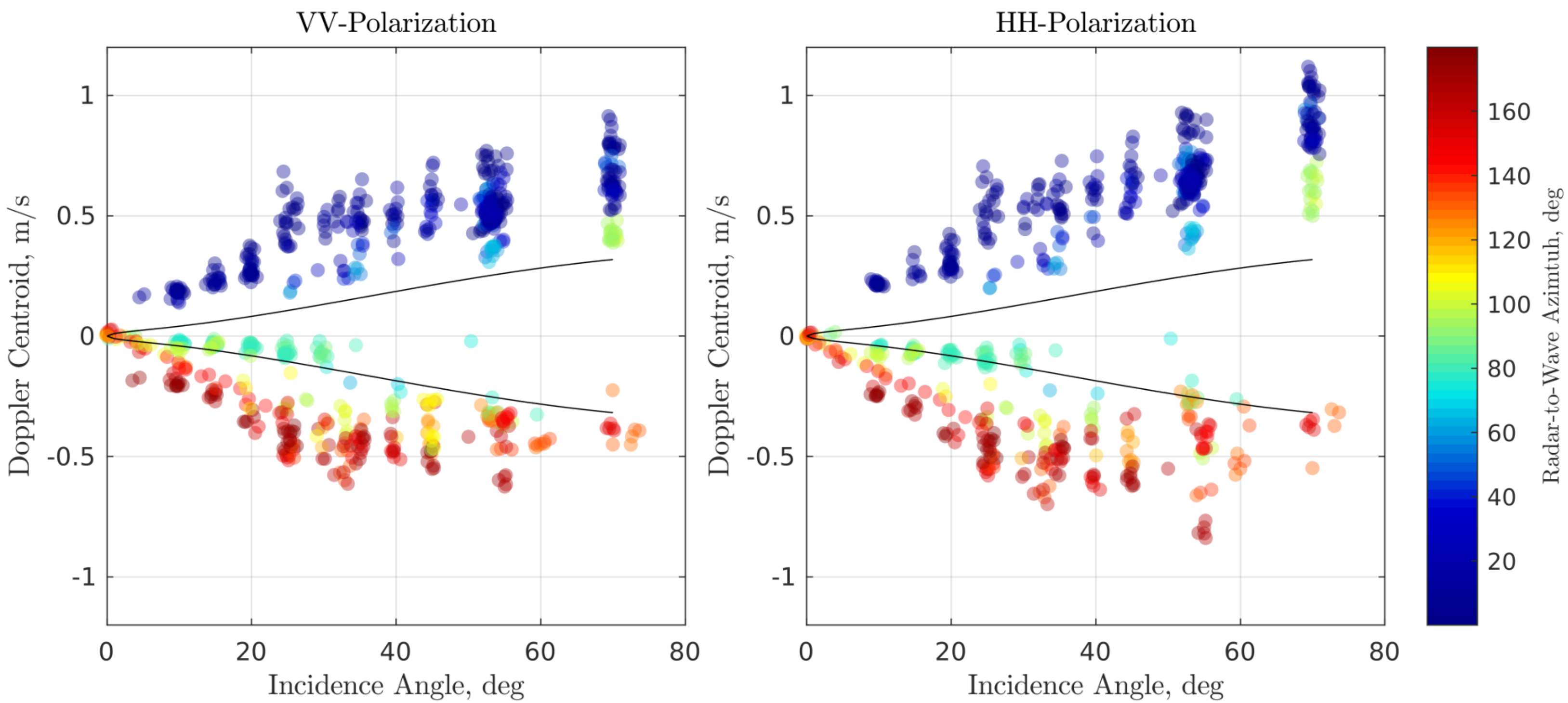

- The most naive “pure Bragg” is totally lower

Doppler Centroids

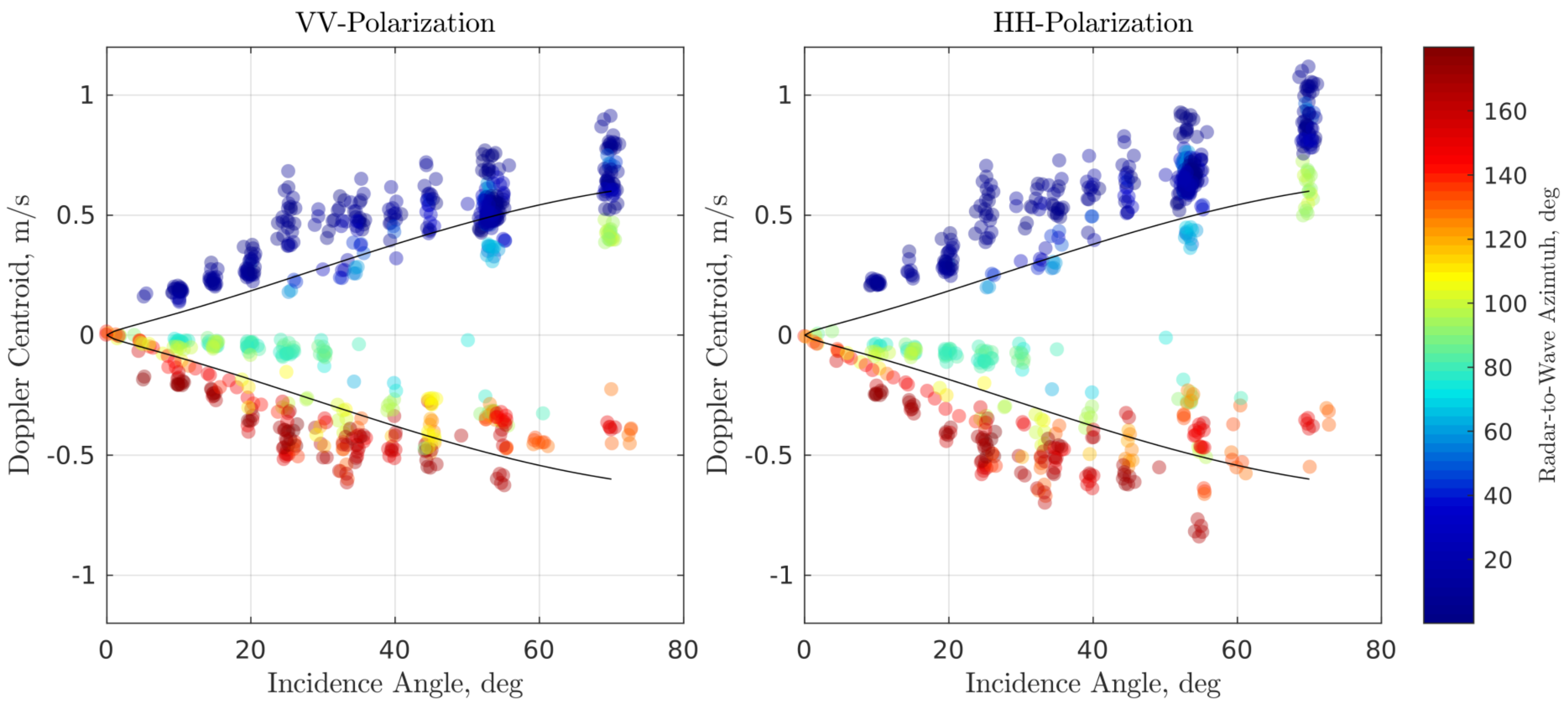

- Adding the wind drift, 3% of U10=10m/s which is much more than average U10 for our data cloud, does not explain the DC

Doppler Centroids

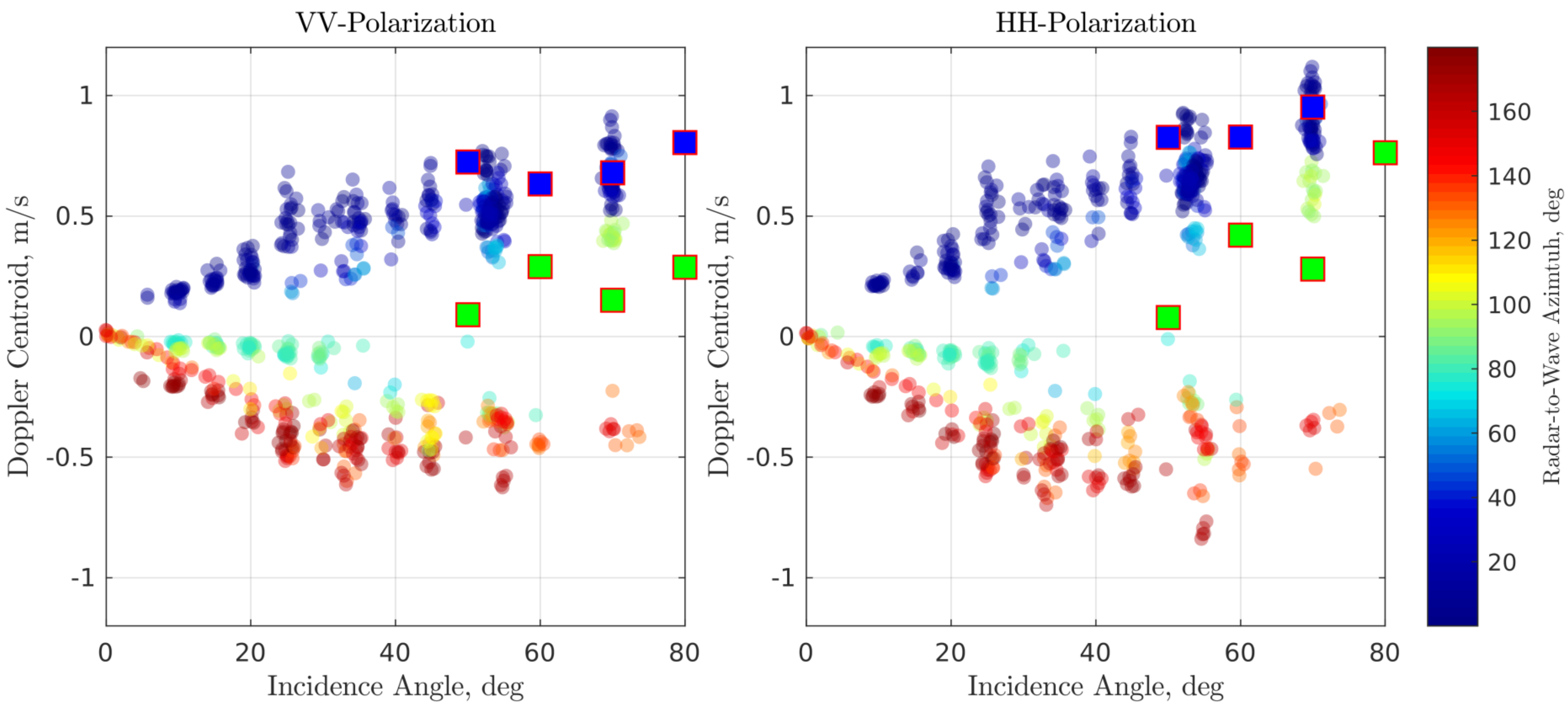

- Plant 1997 JGR: FPN experiment data, X-band, estimated manually
- Strong DC excess in cross-wind → expected DC bias

Doppler Centroids

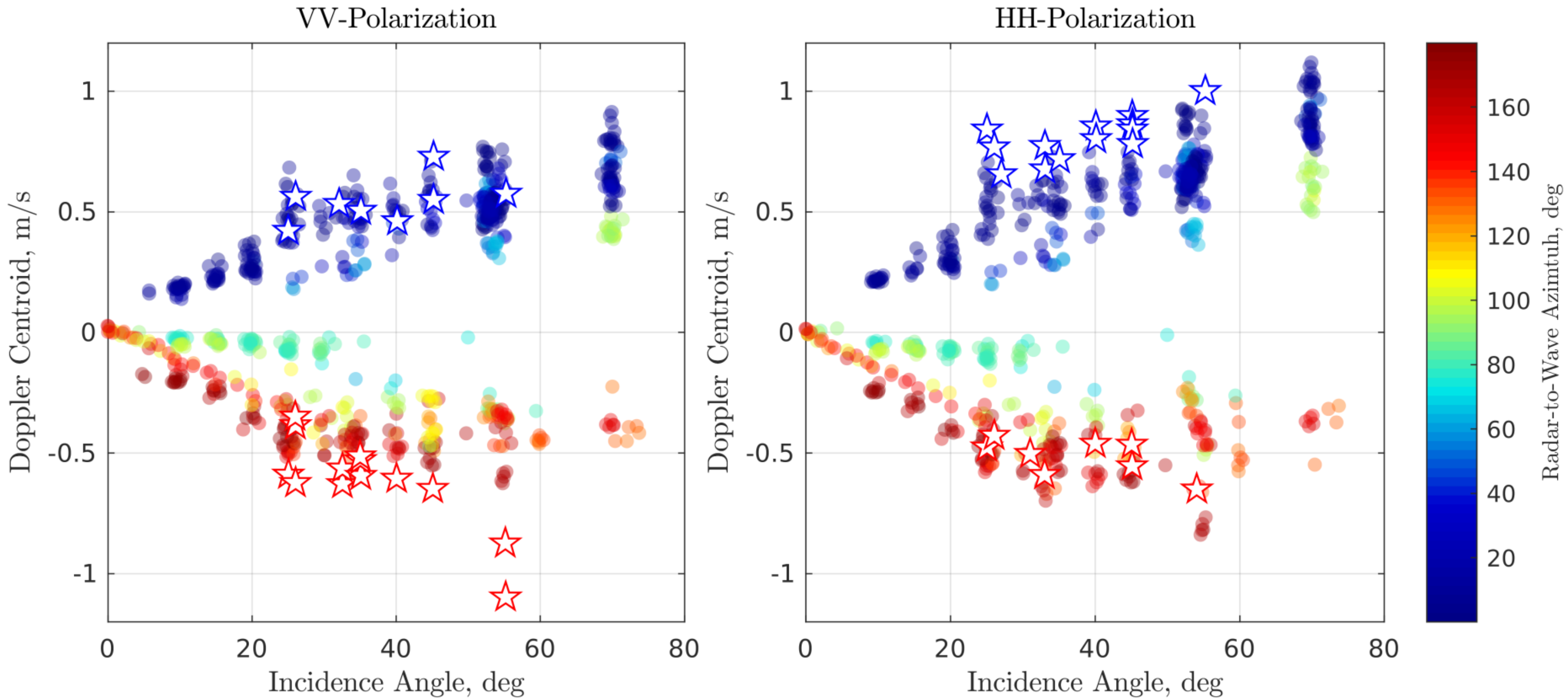

- Ermakov et al. 2014: the same platform, X-band, only upwind and downwind, VV and HH
- Some systematically higher HH-upwind and VV-downwind

Doppler Centroids

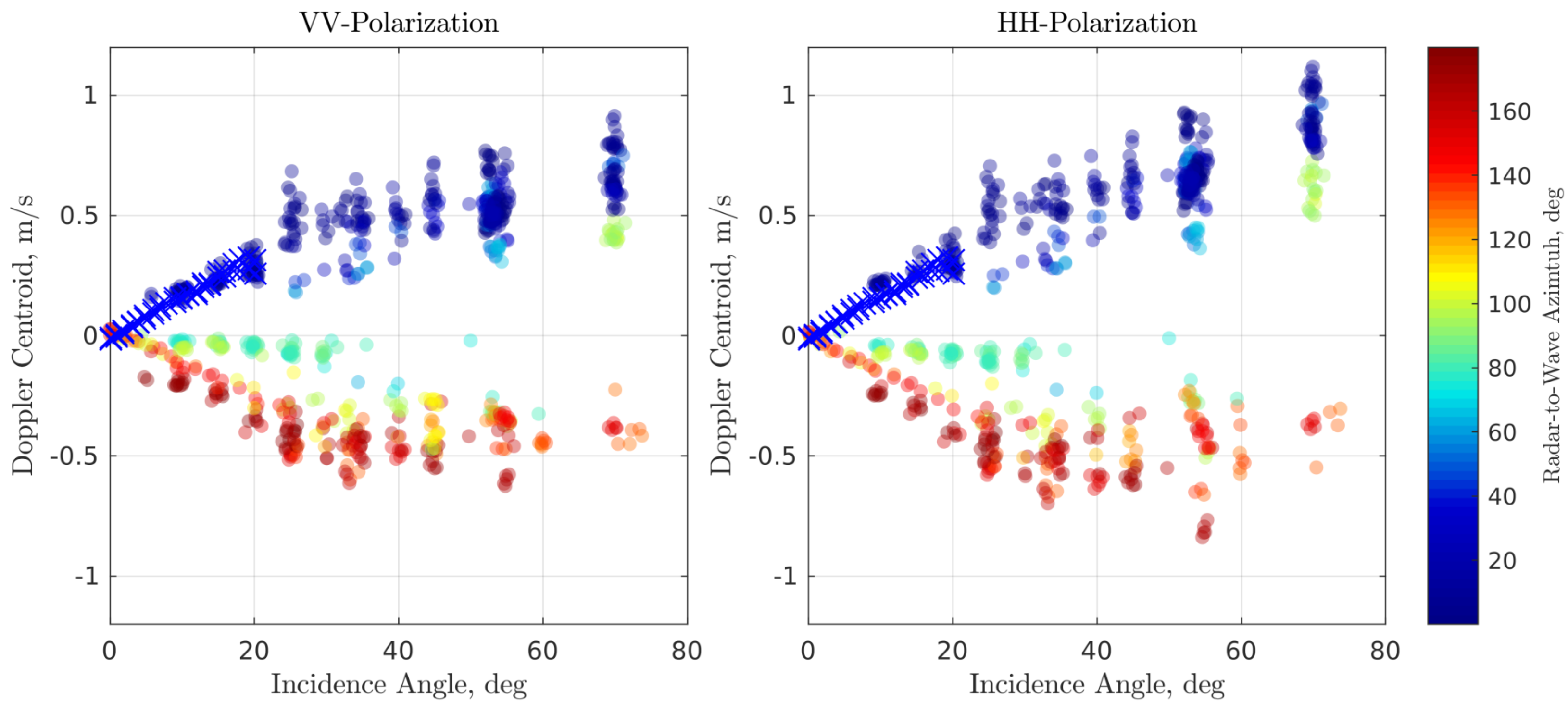

- Karaev et al. 2017: the same platform, Ka-band, only light winds (3-4 m/s), near upwave azimuth
- Good agreement, but no data at strong winds (large waves)

Doppler Centroids

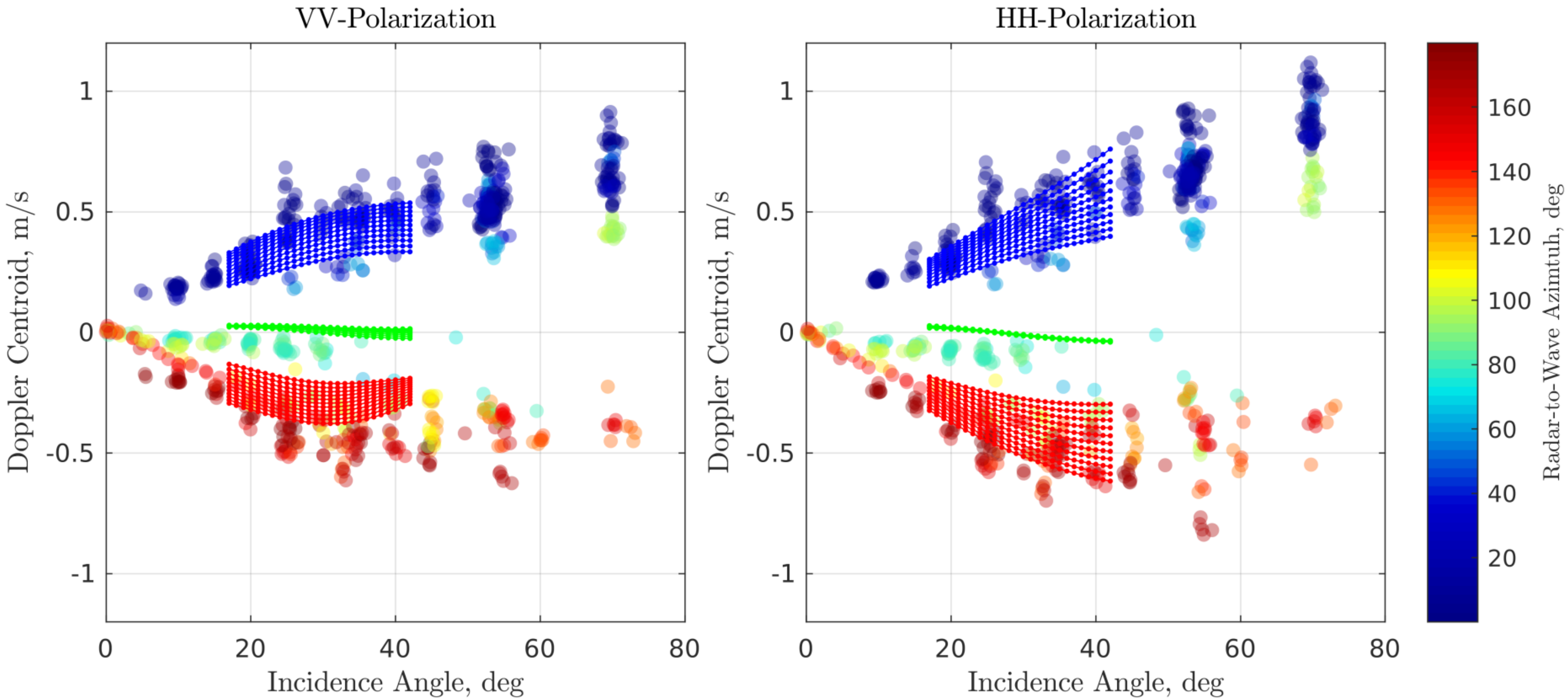

- Mouche et al. 2012: CDOP empirical model, C-band, lines correspond to winds from 5 to 15 m/s
- Good agreement for mean DC levels with some strange behaviour at VV downwind.

Doppler Centroids

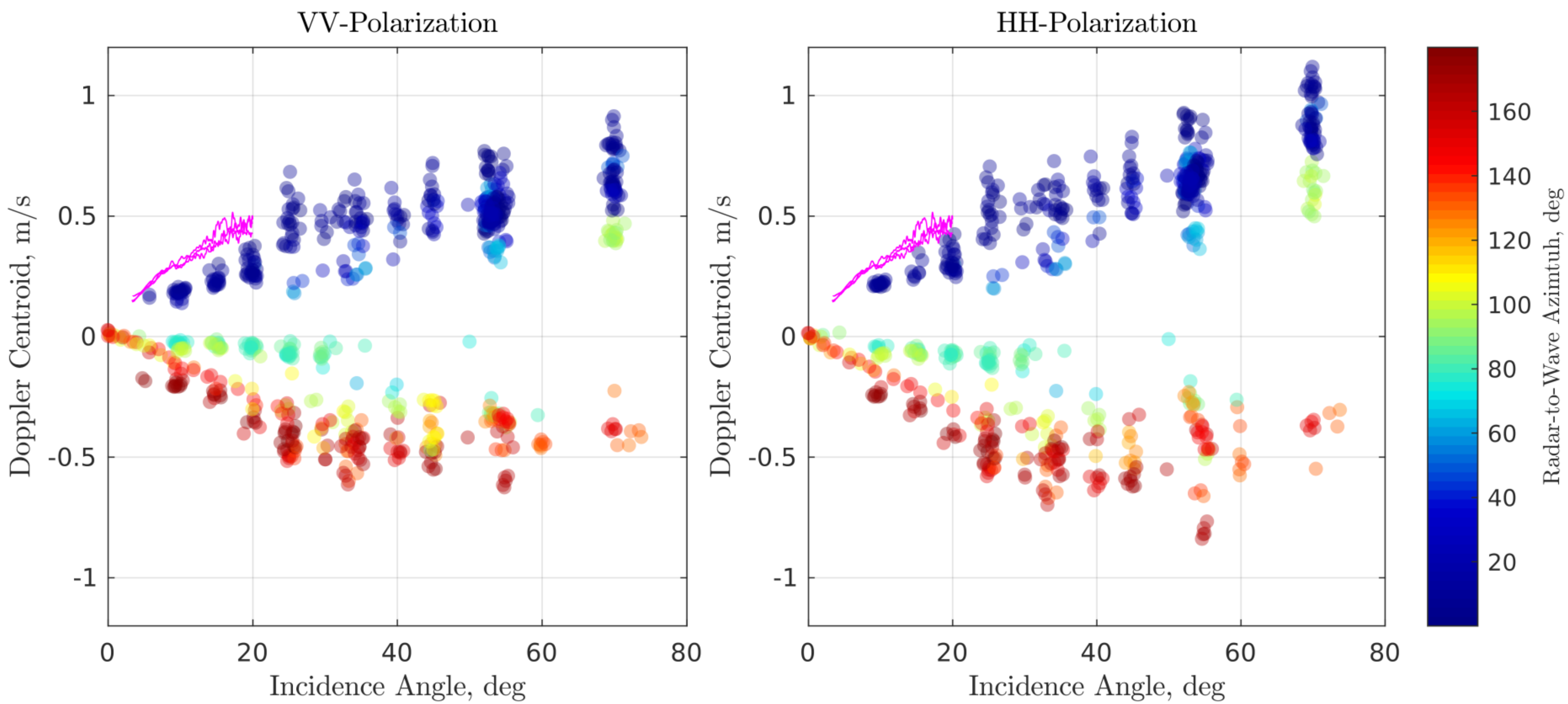

- Nouguier et al. 2018: AirSWOT data, Ka-band, 8 m/s wind speed, 40-m wavelength, non-well developed wind sea
- The same trend, but higher values due stronger winds

Doppler Centroids

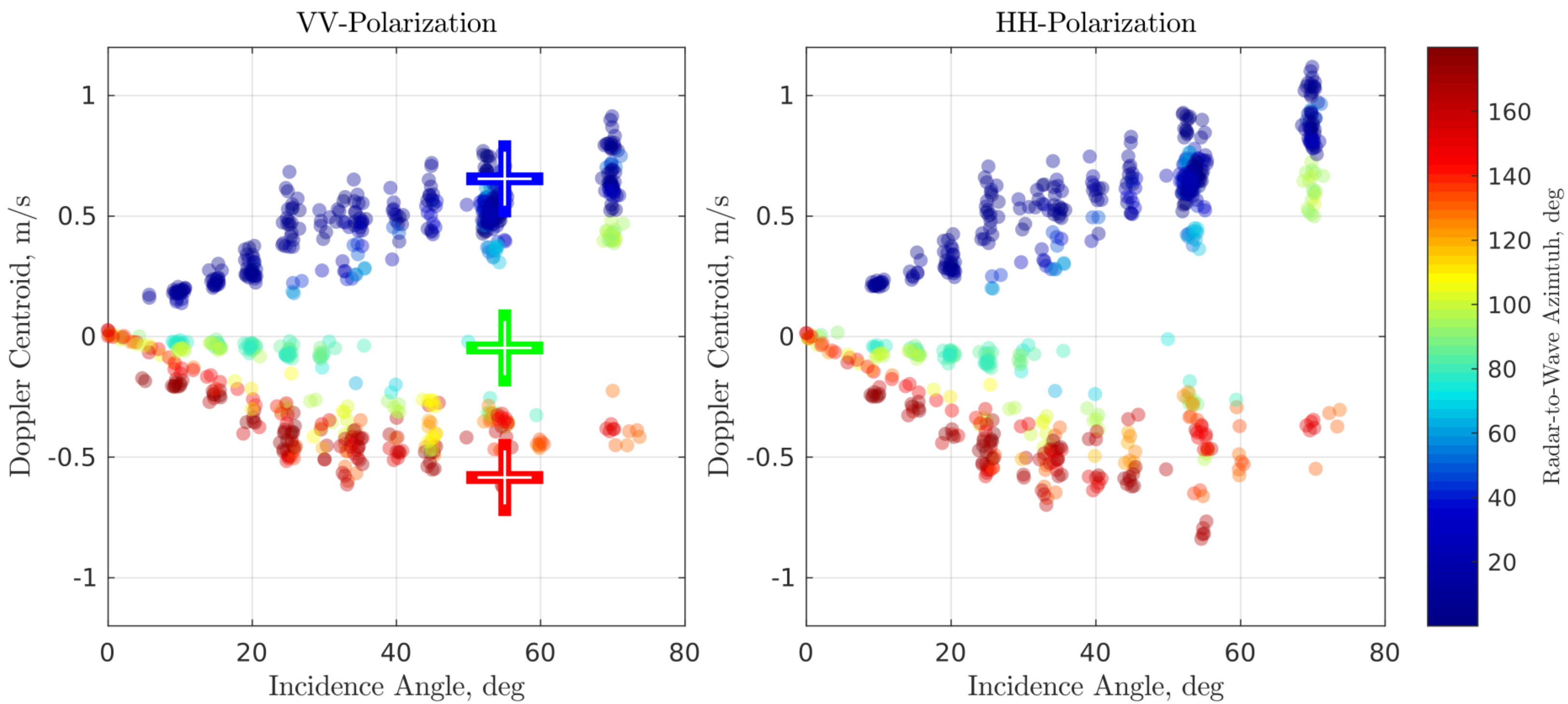

- Rodriguez et al. 2018: DoppScatt GMF data, Ka-band, VV-polarization only, 10 m/s wind speed is shown
- Good agreement, with a bit higher downwind DC magnitude → platform shadowing

Summary

- The MHI platform provides favorable conditions for the Doppler measurements in a well-controlled field conditions
- Empirical models for the NRCS and MTF are proposed
- Both can be used for estimation of the wave-induced Doppler bias depending on look geometry and sea state
- Wave breaking signatures in Doppler velocity are not that strong as in the cross-section (good news for the current retrieval from Doppler?)
- Doppler centroid measurements are in good agreement with available data, but provide more continuous estimates in various sea states and wider look geometries that can be used in the planning of future ocean Doppler-based sensors.

RSF | Russian Science Foundation

Supported by RCSF grant 17-77-10052